Friction

Review Article

Gear contact fatigue: Models and tests

Huaiju Liu[1,✉], Xiuhua Zhang[1], Michael Geitner[2], Thomas Tobie[2], Karsten Stahl[2], Caichao Zhu[1]

Cite this article: Liu HJ, Zhang XH, Geitner M, et al. *Friction* 2026, **14**(1): 9441078. https://doi.org/10.26599/FRICT.2025.9441078

ABSTRACT: The rapid evolution of advanced equipment that utilizes gears, including aviation engines, helicopters, and wind turbines, imposes escalating demands for enhanced reliability, prolonged lifespan, increased power density, and sustained durability of gears. Gear contact fatigue issues, associated with materials, geometries, and operating conditions, are crucial to modern gear design. To date, enormous theoretical and experimental studies have been conducted to understand gear contact fatigue mechanisms. To compile and categorize key investigations within a broad and active research field, this work reviews recent studies of gear contact fatigue. Emphasizing theories, tests, and anti-fatigue design approaches, this work aims to provide a comprehensive overview of recent developments in this significant area of research.

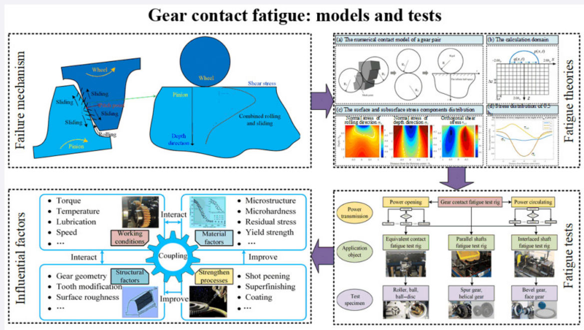

KEYWORDS: gears; contact fatigue; fatigue theories; fatigue experiments; surface integrity

1 Introduction

High-strength gears [1] are critical mechanical elements of advanced equipment such as aviation engines, vehicle reducers, and wind turbine gearboxes. They are confronted with industrial challenges of higher loads (⩾ 3 GPa), speeds (⩾ 20,000 r/min), and temperatures (⩾ 200 °C). These factors lead to various gear failures, including contact fatigue [2, 3] (e.g., pitting [4], micropitting [5], and tooth flank fracture (TFF) [6]), bending fatigue [7, 8], wear, and scuffing [9]. Of these, gear contact fatigue arises from multiaxial, time-varying, and nonproportional stresses in the surface and subsurface areas. The failure mechanisms of gear contact fatigue are complicated because of factors such as geometry, operating conditions, lubricants, materials, and surface integrity parameters. Accidents induced by gear contact fatigue are of nonnegligible concern to human and machine safety and are frequently experienced in engineering practice. A survey conducted by the Japan Society of Mechanical Engineers (JSME) on gear failures in many industries revealed that the percentage of gear surface failures accounts for approximately 74% [10]. The statistical data of gear fatigue failures collected from seventy main reducers of automotive rear axles indicated that approximately 37% of these failures were attributed to gear contact fatigue [11]. Figure 1 shows typical forms of gear contact fatigue failure commonly observed in the aviation, wind turbine, and heavy-duty vehicle industries. For the conformal gear tooth of a helicopter, micropitting and macropitting are primarily caused by an inadequate lubrication film thickness [12]. The tooth flank fracture of a wind turbine gear mainly results from subsurface inclusions [13]. Micropitting is particularly common in the case of a hardened sun gear of off-highway axles subjected to high loads and poor lubricating conditions [14]. The gear pitting of heavy-duty truck gearboxes is usually generated because of high stress [15].

Over a century-long study on gear contact fatigue, the Hertzian formula has served as a basic methodology for calculating gear contact strength. The gear contact analysis that originated from Hertzian contact theory provides a foundation for various design specifications that are adopted at present [16]. In the early 20th century, the American Society of Mechanical Engineers (ASME) conducted numerous gear material tests, the collected data of which were adopted by the American Gear Manufacturers Association (AGMA) [17]. Moreover, the international standard ISO 6336 [18] was developed for the calculation of the load-carrying capacity of spur and helical gears, which is primarily based on the German standard DIN 3990 and the US standard ANSI/AGMA 2001. ISO 6336 was published in its first edition in 1996. The standard stands at the forefront of gear rating techniques worldwide and is continuously being improved and extended. A technical system that integrates theories, experiments, and designs was subsequently established with the aid of fatigue analysis, mechanical advancement, durability testing, and artificial intelligence (AI). Global research institutions have been increasingly emphasizing the establishment of a gear contact fatigue database to explore gear fatigue data for different materials, manufacturing processes, and geometries. The transition from

[1] State Key Laboratory of Mechanical Transmission for Advanced Equipment, Chongqing University, Chongqing 400030, China. [2] School of Engineering and Design, Gear Research Center (FZG), Technical University of Munich, Garching bei München 85748, Germany.

✉ Corresponding author. E-mail: huaijuliu@cqu.edu.cn

Received: August 8, 2024; Revised: December 18, 2024; Accepted: February 12, 2025

extensive design methodologies that rely on empirical formulae and outdated data to high-power-density gear design approaches promotes the development of gear anti-fatigue technologies. In the gear anti-fatigue technology area, design theories, manufacturing processes, testing approaches, signal measuring, and AI-aided software tools are involved.

Despite substantial advancements in these aspects of gear contact fatigue, challenges remain. The complicated and interactive effects of tooth surface integrity on contact fatigue behavior make it difficult to discover the gear contact fatigue mechanism. Current gear contact fatigue tests demonstrate features such as large loading cycles ($\geqslant 5\times10^7$), large sample sizes (at least 20–25 valid tests for obtaining a complete *S*–*N* curve), and obsolete data processing techniques, making the development of a gear durability database difficult. The design standards for fatigue strength rely on many empirical coefficients and lack comprehensive consideration of surface integrity, leading to significant challenges in ensuring the high power density of gear machines.

With more demanding requirements being proposed by industry, the present work reviews relevant studies on gear contact fatigue, including theoretical and experimental methods, influencing factors, and gear anti-fatigue design methodologies. In addition, recent results obtained by the authors are presented and discussed as supporting evidence.

2 Gear contact fatigue failure mechanism

Gear contact fatigue is one of the primary failure modes occurring even under the conditions of proper installation, loading, and lubrication. It initiates on or near the tooth surface under cyclic contact loading. As shown in Fig. 2, gear contact fatigue failure that initiates from the surface can be distinguished as micropitting or (macro)pitting. Moreover, TFF also results from contact fatigue, where the critical failure position is at a greater depth from the surface than pitting and micropitting [6]. Of these two surface failures, pitting predominates in gear contact fatigue failure [19]. Practical experiences reveal that micropitting gradually develops into pitting or reaches a stable state without catastrophic failure [20–22]. Consequently, they are collectively termed surface contact fatigue in this work.

Despite the multiaxial and time-varying features of the loading behavior observed in gear contact fatigue, it is widely acknowledged that contact fatigue can be attributed to the maximum Hertzian contact shear stress. This mainly arises from the combined influence of alternating contact stress under relative rolling–sliding motion [23, 24]. Figure 3 shows the rolling–sliding contact between the gear tooth surfaces [25]. A mating gear tooth surface can be regarded as the contact between an elastic cylinder with an equivalent curvature radius and a semi-infinite flat surface, leading to a small local contact area that results in high shear stress close to the surface. On the basis of the depth at which the maximum shear stress occurs, fatigue cracks can be categorized as either surface-originated or subsurface-originated. The initiation depth of surface-originated fatigue cracks is typically within a range of 10–20 μm, which is attributed to various factors, such as surface scratches, surface morphology, and inadequate lubrication. With a high-quality surface and adequate lubrication conditions, subsurface-originated fatigue cracks become the predominant failure mode.

Fatigue crack behavior to failure can generally be divided into three stages: crack initiation, propagation, and ultimate failure. Crack initiation accounts for the majority of the failure process. The orientation of the cracks initiated at the surface is against the

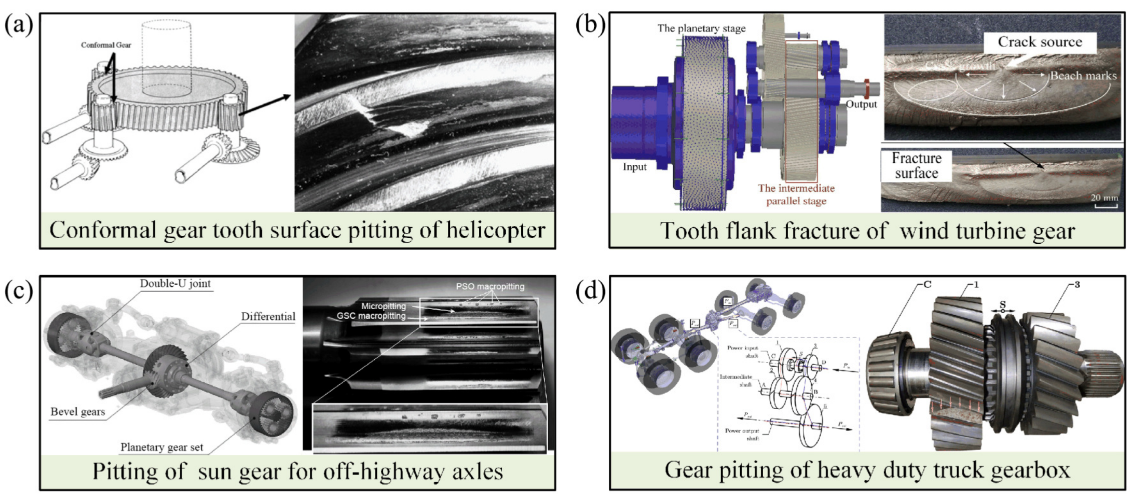

Fig. 1 Typical gear contact fatigue failures in industry. Reproduced with permission from Ref. [12] for (a), © Elsevier Ltd. 2013; from Ref. [13] for (b), © Elsevier Ltd. 2022; from Ref. [14] for (c), © Elsevier Ltd. 2017; from Ref. [15] for (d), © Elsevier Ltd. 2023.

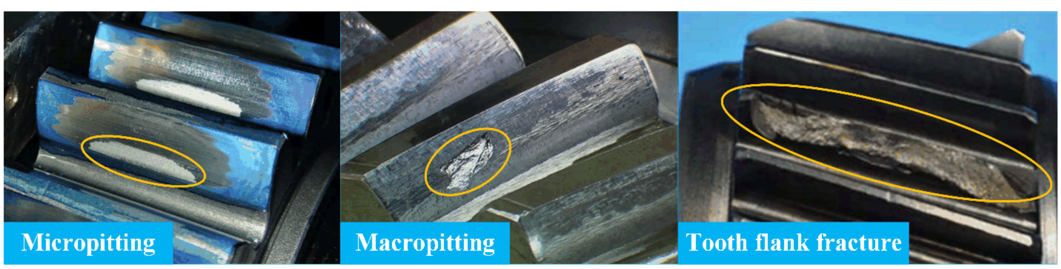

Fig. 2 Gear micropitting, pitting, and tooth flank fracture. Reproduced with permission from Refs. [20, 21], © ISO 2022.

sliding direction. Following crack initiation, the crack typically propagates a short distance along a path nearly parallel to the tooth surface before turning or branching to the surface. A pit will then form when the cracks have grown long enough to separate a piece of surface material. Because the slide direction reverses as the pitch line is crossed, pitting cracks grow in opposite directions above and below the pitch line along the line of action (LOA). The pit edges are usually sharp and angular. Cracks can be found near the edges of the pit, and fatigue "beach marks" are sometimes evident on the crater bottom. The original pits are small compared with the size of the contact zone. Spalling occurs when small pits coalesce and form irregular craters that cover a significant area [20, 21].

The evolution of gear contact fatigue is influenced by many factors, including surface morphology, gear geometry, material strength, and operating conditions. Sharif et al. [26] studied the effect of surface roughness on gear fatigue failure via a mixed lubrication model. Liu et al. [27] conducted a study on the influence of residual stress on pitting crack initiation and propagation life, with the fatigue *S*–*N* curve predicted by utilizing various multiaxial fatigue criteria. They concluded that the Zaretsky model is more suitable for gear life evaluation under multiaxial stress states. Li and Kahraman [28] evaluated the crack initiation life under rolling contact conditions by considering the influence of lubrication on the contact state. Li and Anisetti [29] studied the effect of dynamic loads on gear fatigue and proposed a contact fatigue model coupling gear tribology and dynamics. The specific influence of each factor is presented in Section 5. With respect to pitting control, corresponding design specifications, such as ISO 6336, AGMA 2101, DIN 3990, and GB/T 3480, have been published.

3 Gear contact fatigue theories

3.1 Prediction methods for gear contact fatigue life

(1) Statistical fatigue life prediction models

Numerous statistical models for predicting gear contact fatigue life have been established over the past few decades, as shown in Fig. 4. The contact state similarity between gears and bearings prompted the initial application of the Lundberg–Palmgren (L–P) model [30] for gears, which is predominantly used in rolling bearing contact fatigue assessment. The L–P model proposed that pitting occurrence can be attributed to the unequal distribution of high contact stress. In 1975, Coy and Zaretsky [31] experimentally confirmed that the L–P model can be extended to apply to gears. They formulated a formula shown in Eq. (1) to predict the gear contact fatigue life.

$$L_{10} = \left(\frac{K z_0^h}{\tau_0^c V} \right)^{\frac{1}{e}} \tag{1}$$

where L_{10} is the fatigue life with a reliability of 90%; K is a material

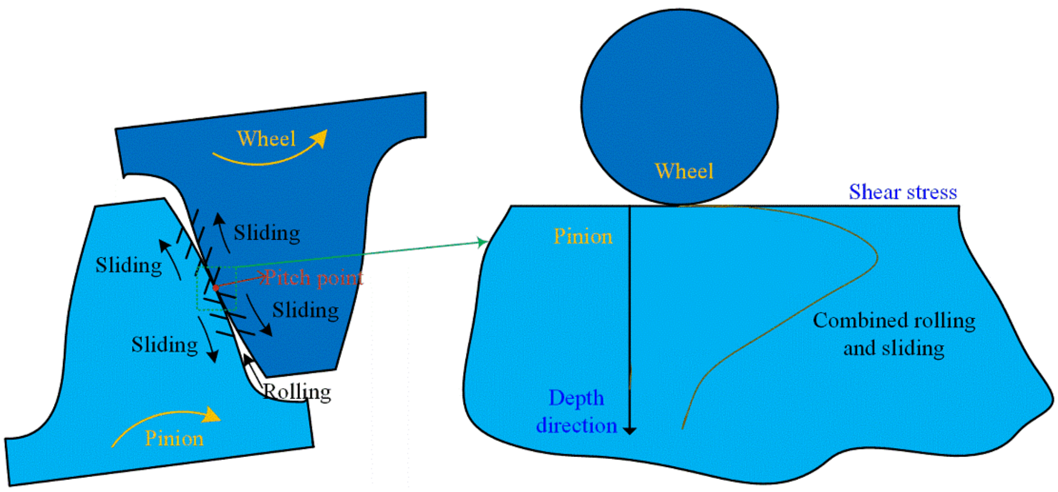

Fig. 3 Rolling–sliding contact between gear tooth surfaces [25].

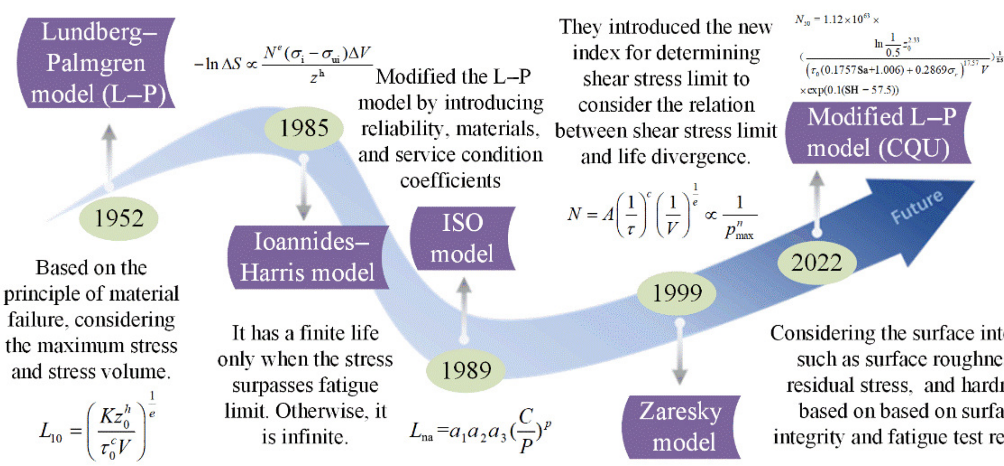

Fig. 4 Development of statistical models for gear contact fatigue life.

parameter that determines the load-carrying capacity for a single tooth of pinion; V is the volume of the high-stress area; z_0 is the stress volume depth; c is the stress index; h is the depth index; τ_0 is the maximum orthogonal shear stress; e is the Weibull distribution slope parameter of the tested life.

The evolution of strengthening technologies, such as shot peening and surface finishing, has resulted in significant improvements in gear surface integrity. Consequently, the adaptability of the original L–P model has become constrained because of its poor applicability for surface-strengthening components. To address this issue, a modified L–P model that accounts for surface integrity was proposed on the basis of fatigue test results by Zhang et al. [32]. The proposed formula, named the modified L–P model (CQU), enables a more accurate and reliable estimation of the gear fatigue life with surface strengthening, as shown in Fig. 5.

To overcome the limitations of the L–P model, notably disregarding the tangential stress, Ioannides and Harris [33] discretized the stress region into discrete material points. It is posited that fatigue failure would only occur if the stress exceeded the fatigue limit. However, Zaretsky et al. [34] argued that introducing a fatigue limit could result in an overestimation of fatigue life. Through an extensive review, they discovered that the parameter c/e served as the most effective index for determining the shear stress limit and modified the L–P model. Equation (2) shows the modified L–P model by Zaretsky et al [34].

$$N = A\left(\frac{1}{\tau}\right)^{c}\left(\frac{1}{V}\right)^{\frac{1}{e}} \propto \frac{1}{p_{\max}^{n}} \tag{2}$$

where $p_{\max}$ is the maximum Hertzian contact stress and n is the index of the maximum Hertzian contact stress, which can be determined based on the Hertzian contact theory.

In addition, other statistical models, such as the ISO model [35] and the Chiu–Tallian model [36], have been developed. The methodologies and unique features of these methods are described in Ref. [32]. Over the years, statistical approaches for predicting gear contact fatigue life and limits have made significant advancements. However, the complex nature of the gear contact and damage process has resulted in several limitations of these statistical models, including the use of many empirical coefficients and the lack of consideration of factors such as the oil film state, material nonhomogeneity, and residual stress.

(2) Deterministic fatigue life prediction models

Deterministic fatigue life prediction models employ finite element analysis or other techniques to obtain the stress–strain response. The fatigue criteria are subsequently used to predict the gear contact fatigue life. One of the factors that complicates contact fatigue is the surface and subsurface stress states during rolling–sliding contact. The stress states in nonconformal contacts are complex and multiaxial, which is a determinant of contact fatigue and difficult to predict via Hertzian contact theory. The finite element method, as a representative numerical simulation technique, enables the resolution of complex stress states by discretizing the tooth into a finite number of nonoverlapping elements. Within each element, an approximation of the true solution is achieved through the combination of element basis functions. Figure 6 depicts the distributions of surface and subsurface stress components at the pitch point via numerical simulation [27], elucidating multiaxial features, where b_{H} represents the half Hertzian contact width at the pitch point. The stress components do not vary with time in the same proportion. There is an obvious reversal of the orthogonal shear stress, whereas the normal stresses in the rolling direction and depth direction always remain compressive. In addition, the tooth subsurface endures a non-proportional cycle of tensile stress, shear stress, and compressive stress during gear meshing, leading to time-varying principal stress and strain orientations. This phenomenon complicates the identification of initiation sites and propagation directions for fatigue cracks.

Early numerical models for gear contact fatigue primarily relied on several assumptions, including smooth surfaces and uniform material characteristics, while critical surface integrity factors such as surface morphology, hardness, and residual stress were neglected. To overcome this difficulty, Wang et al. [37, 38], Liu et al. [39], and Wei et al. [40] dedicated efforts toward developing a gear contact numerical model that considers surface integrity, providing a methodological foundation for gear fatigue analysis. The asperity contacts because the micro peaks and valleys of the tooth surface significantly increase the local contact pressures, resulting in pronounced stress concentrations and an increased risk of fatigue crack initiation. The realization of rough surface contact fatigue analysis depends on the acquisition of real surface morphologies. The surface morphology can be measured through contact methods, optical methods, and scanning electron microscopy. The hardness gradient of a gear tooth can be measured via microhardness tests and nanoindentation instruments. In numerical models, consideration of the hardness gradient is typically achieved via the conversion correlation between hardness and yield strength [41]. Optical, mechanical, and diffraction methods are commonly used to measure gear residual stress. The residual stress profile can then be incorporated into numerical models through a predefined stress field setting. The material microstructure was measured through scanning

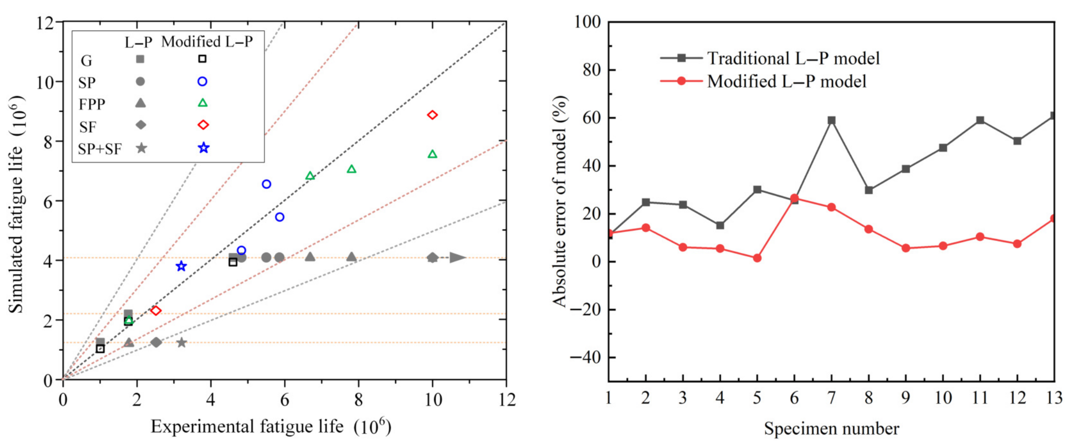

Fig. 5 Comparison of predicted results between modified L–P model and traditional L–P model. Reproduced with permission from Ref. [32], © The author(s) 2022.

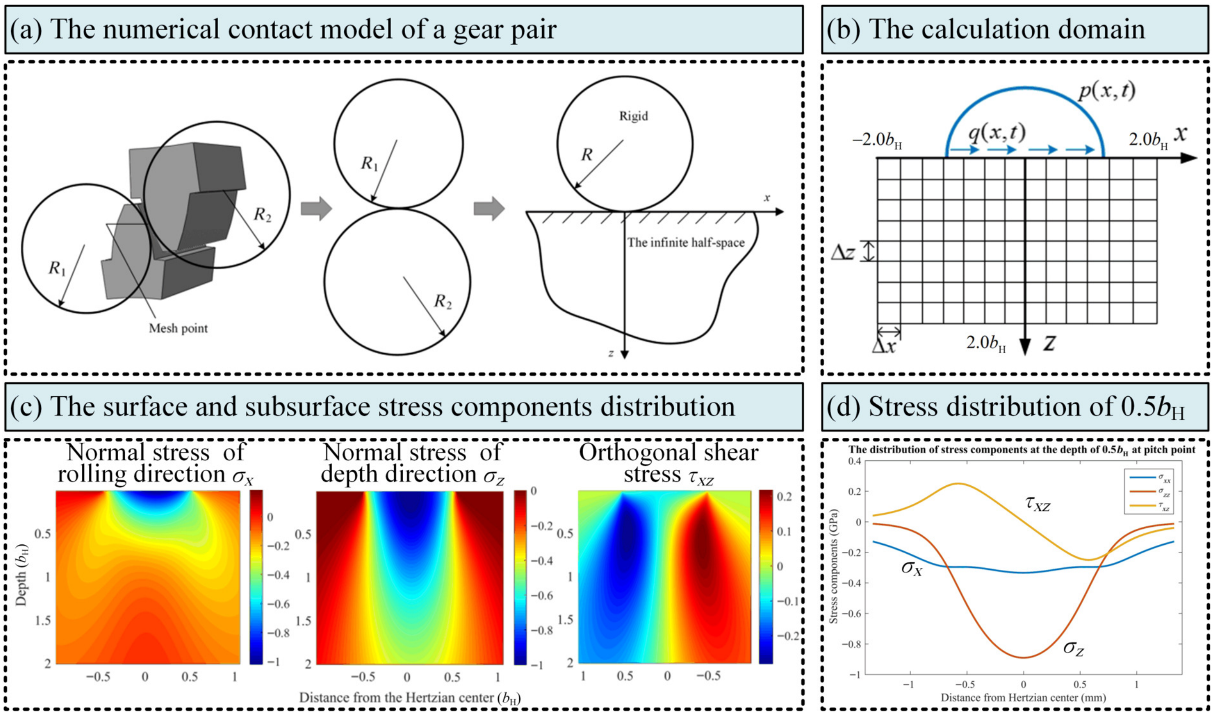

Fig. 6 Distributions of surface and subsurface stress components at pitch point for a gear pair. Reproduced with permission from Ref. [27], © The American Society of Mechanical Engineers 2018.

electron microscopy, transmission electron microscopy, or electron backscatter diffraction. The procedures used to model material microstructures include image processing, grain reconstruction, and property assignment. To simulate tooth flank fracture, another typical gear contact fatigue failure, in addition to pitting and micropitting, it is necessary to consider material inclusions in the subsurface and core areas.

The meshed tooth surface typically exhibits elastic–plastic deformation, particularly at the micrometer scale. A typical elastic–plastic constitutive equation for metal materials comprises yield criteria, hardening models, and flow rules. The predominant yield criteria for gear materials include the maximum principal stress theory [42], the maximum principal strain theory [43], the maximum shear stress theory [44], and the von Mises stress yield criterion [45]. These criteria are frequently utilized for determining the location of crack initiation. Common plasticity mechanics typically incorporate several hardening models, namely, the isotropic hardening model, the kinematic hardening model, and the mixed hardening model. Among them, the kinematic hardening model is particularly pertinent, and the Chaboche model [46] and Jiang–Sehitoglu model [47] are notable examples that possess extensive applicability for carburized gear steels. The stress history can be determined by the flow rule.

Multiple axial and time-varying stress states are observed in the tooth contact area, so numerous fatigue criteria have been developed. The critical plane-based multiaxial fatigue criterion has attracted increasing interest. The Brown–Miller (B–M) [48], Fatemi–Socie (F–S) [49], and Dang–Van (D–V) [50] criteria have been used by researchers. According to the B–M criterion, fatigue crack initiation occurs on the plane with the highest shear strain. The critical plane is subjected to both shear and normal strains that affect the fatigue process together. The mathematical formulation for this criterion is shown as Eq. (3) [51]:

$$\frac{\Delta\gamma_{\max}}{2} + S\Delta\varepsilon_{\mathrm{n}} = A\frac{\sigma'_{\mathrm{f}}}{E}(2N_{\mathrm{f}})^{b} + B\varepsilon'_{\mathrm{f}}(2N_{\mathrm{f}})^{c} \tag{3}$$

where $\Delta\gamma_{\max}$ and $\Delta\varepsilon_{\mathrm{n}}$ are the amplitudes of the maximum shear strain and the normal strain, respectively; $2N_{\mathrm{f}}$ is the fatigue life; b and c are the fatigue strength exponent and the fatigue ductility exponent, respectively; σ'_{f} and ϵ'_{f} are the fatigue strength coefficient and the fatigue ductility coefficient, respectively; S is the material constant.

The B–M criterion is widely used to estimate the fatigue life of ductile metals. It is considered to be the preferred method for predicting fatigue behavior in conventional materials. Nonetheless, a study conducted by Fatemi and Socie [52] demonstrated that relying solely on strain parameters may fail to account for the significant strengthening effect under non-proportional loading conditions. The F–S model was proposed to address this limitation by incorporating normal stress components, as given by Eq. (4):

$$\frac{\Delta\gamma_{\max}}{2}\left(1+k\frac{\sigma_{\max}}{\sigma_{\mathrm{ys}}}\right) = \frac{\tau'_{\mathrm{f}}}{G}(2N_{\mathrm{f}})^{b} + \gamma'_{\mathrm{f}}(2N_{\mathrm{f}})^{c} \tag{4}$$

where $\sigma_{\max}$ is the maximum normal stress; σ_{ys} is the yield strength of the material point; τ'_{f} and γ'_{f} denote the shear fatigue strength coefficient and shear fatigue ductility coefficient, respectively; k, G, and c are constants related to the contact stress and material.

The F–S model has demonstrated high accuracy in predicting fatigue behavior under nonproportional loading conditions. Wang et al. [37, 53] created a crystal plasticity finite element model for wind turbine gears. This model considers the F–S multiaxial fatigue criterion and simulated stress and strain behaviors in the slip system and fatigue damage at the grain level. They calculated the gear contact fatigue life considering both the compressive residual stress and the hardness gradient along the depth. While the F–S and B–M models are capable of fatigue life prediction in some cases, their suitability is restricted to finite-life designs. Consequently, models such as the Crossland and D–V models emerged successively, offering possibilities for designing an infinite life. Reis et al. [54] predicted the fatigue crack initiation behavior of rail materials subjected to random loading via the D–V model. Furthermore, the multiaxial fatigue criteria also include the Jiang–Saghulu [55], Matake [56], and Findley formulae [57]. Each of these criteria varies in terms of scope, factors considered, and prediction accuracy, allowing people to select what is most suitable for their particular needs.

The following is a case study regarding the prediction of gear contact fatigue life via the deterministic model [27]. In this study, a deterministic model is introduced to assess the contact fatigue life of wind turbine gear pairs. Discrete convolution and fast Fourier transform methods are utilized to estimate subsurface stress distributions. Multiple axial fatigue criteria are applied to determine the equivalent stresses and evaluate the fatigue life. The impact of residual stress distributions on fatigue life is discussed. These findings reveal that residual stress influences equivalent stresses, thereby significantly affecting gear contact fatigue life.

3.2 Prediction methods for gear contact fatigue strength

It is essential to assess gear contact fatigue strength, which is the maximum contact stress that a gear can withstand under infinite cyclic loading, for ensuring reliable gear design. The gear industry has conducted studies on gear contact fatigue strength, creating many prediction methods. These methods have been incorporated into several widely accepted industrial specifications, including ISO 6336, AGMA 2101-D04, DIN 3990-2, and GB 3480. Figure 7 shows a fundamental calculation procedure for the gear contact fatigue strength. Equations (5) and (6) for permissible contact stress can be found in ISO 6336-2 [18]. The permissible contact stress is the maximum stress that can be applied to the tooth surface.

$$\sigma_{\mathrm{HP}}=\frac{\sigma_{\mathrm{Hlim}}}{S_{\mathrm{Hlim}}}Z_{\mathrm{NT}}Z_{\mathrm{L}}Z_{\mathrm{v}}Z_{\mathrm{R}}Z_{\mathrm{W}}Z_{\mathrm{X}} \tag{5}$$

$$\sigma_{\mathrm{H}}\leqslant\sigma_{\mathrm{HP}} \tag{6}$$

where σ_{Hlim} is the gear contact fatigue strength limit of the standard reference test gears; S_{Hmin} is the minimum required safety factor for surface durability; Z_{NT} is the life factor; Z_{L} is the lubricant factor; Z_{v} is the velocity factor; Z_{R} is the surface roughness factor; Z_{W} is the work hardening factor; Z_{X} is the size factor.

The prediction formula for gear permissible contact stress used in AGMA 2101-D04 is given by Eq. (7) [58]:

$$\sigma_{\mathrm{HP}}=\frac{\sigma_{\mathrm{Hlim}}}{S_{\mathrm{Hlim}}}\frac{Z_{\mathrm{NT}}Z_{\mathrm{W}}}{Y_{\theta}\,Y_{\mathrm{Z}}} \tag{7}$$

where Y_{θ} is the temperature factor and Y_{Z} is the reliability factor.

The DIN 3990-2 [59], GB/T 3480 [60], and ISO specifications are substantially similar. Both the ISO and AGMA specifications are founded on Hertzian contact theory and consider a range of correction coefficients, resulting in comparable formats. Compared with the AGMA standard, the ISO standard considers a wider spectrum of factors related to permissible stress. ISO highlights the lubrication performance through lubrication coefficients, whereas AGMA incorporates temperature coefficients for the same purpose. The fatigue limit predictions and tests differ because of the varying gear parameters, materials, and heat treatments used [58, 61]. Compared with ISO 6336, AGMA 2101-D04 is more dependent on the tooth module, tooth number, pressure angle, and tooth profile. Labath and Richter [62] proposed that changes in the tooth profile, helix angle, and pressure angle lead to different results for the ISO and AGMA. The implementation of diverse correction factors can give rise to inconsistencies in strength calculations. The majority of studies indicate that the ISO method yields more conservative results [63, 64] because of discrepancies in stress cycle coefficients, uneven load distribution coefficients, and fatigue limit parameters. Gear designers may choose between different methods and standards when designing gears. For example, designers may select the ISO specification if there are stringent safety requirements or inadequate experience in new applications. For the conventional gear design, the AGMA specification may be selected because of its expedient and straightforward computations. In addition, ISO/TS 6336-22 represents a rating method that considers micropitting on the basis of the specific lubricant film thickness and the micropitting resistance, which is evaluated in a standardized test according to DIN 3990-16 [65] and FVA 54/7 [66].

3.3 Data-driven models for gear contact fatigue performance

Gears sometimes encounter failures such as contact fatigue within their design lives. The major reason is that the effects of surface morphology, hardness gradient, lubrication properties, etc., are merely coarsely adjusted via coefficients in the formulae. To meet the requirements of high-performance gear design, a quantitative method for evaluating gear fatigue that considers surface integrity

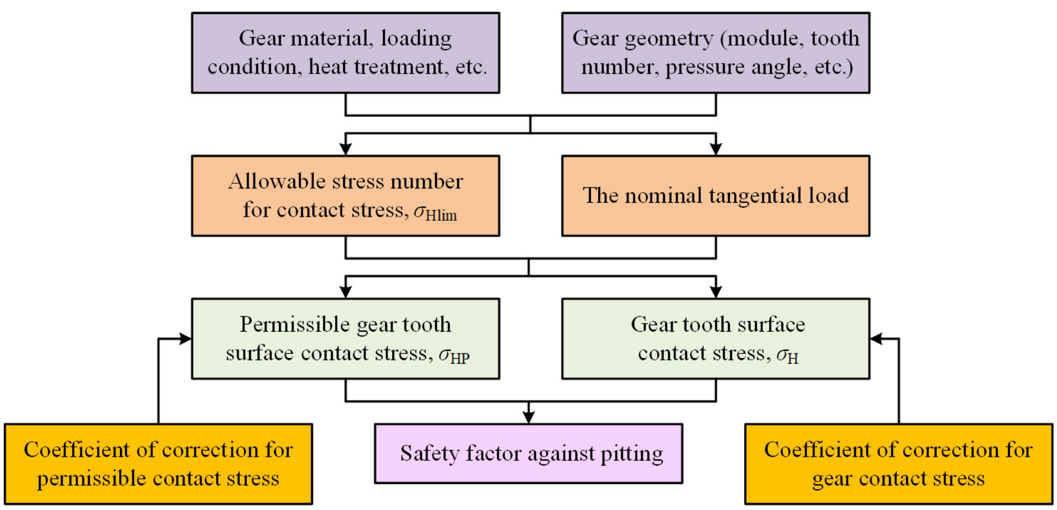

Fig. 7 A fundamental prediction procedure for gear contact fatigue strength.

needs to be established. Based on fatigue test data and artificial intelligence algorithms, the authors devised a data-driven method for predicting gear fatigue. Figure 8 shows the outline for predicting gear fatigue considering surface integrity using data-driven technology.

(1) Parameter selection

People are likely to employ experiential means in parameter selection, inevitably leading to shortcomings, such as inappropriate choices and overly complex models. There are interactions between surface integrity parameters, thus requiring the elimination of multicollinearity between these parameters. Commonly employed correlation analysis methods include the Pearson and Spearman ranks [67, 68]. The Pearson correlation analysis method is employed to assess the strength and direction of the linear relationship between two continuous variables. The Spearman rank correlation analysis method is a non-parametric statistical method used to measure the monotonic relationship between two variables. The closer the absolute value of the correlation coefficient is to 1, the stronger the correlation between the parameters. Conversely, the closer the absolute value is to 0, the weaker the correlation. The corresponding formulae are presented in Eqs. (8) and (9).

$$\rho_{X,Y} = \frac{\sum(X-\bar{X})(Y-\bar{Y})}{\sqrt{\sum(X-\bar{X})^2 \sum(Y-\bar{Y})^2}} \tag{8}$$

$$P_S = 1 - \frac{6\sum d^2}{N(N^2-1)} \tag{9}$$

where $\rho_{X,Y}$ is the Pearson correlation coefficient between two variants or parameters; X and Y are variants, with $\bar{X}$ and $\bar{Y}$ being their average values, respectively; P_S is the Spearman rank correlation coefficient; N is the sample size; d is the difference between two variants and is defined as $X - Y$.

The prevailing belief is that a correlation coefficient with an absolute value exceeding a critical threshold, e.g., 0.8, manifests a strong correlation. When constructing predictive equations for gear contact fatigue performance considering surface integrity, it is advisable to retain one surface integrity parameter while excluding the other, based on this criterion of strong correlation. While the Pearson correlation coefficient demands more rigorous data standards than the Spearman rank correlation coefficient, the Pearson correlation coefficient exhibits a higher calculational efficiency. Thus, people may select the appropriate correlation method for their specific design.

(2) Data-driven model

With the rapid advancement of big data technologies, data-driven approaches, including neural networks, support vector machines, and deep learning, have emerged as prominent trends in performance prediction. Durodola et al. [69] employed a neural network to predict the fatigue damage of metal alloys, yielding superior predictive accuracy. Agrawal and Choudhary [70] utilized data-driven methods to predict the rotary bending fatigue limit under various chemical compositions and heat treatments based on fatigue data from the National Institute for Materials Science (NIMS) Materials Database (MatNavi) (Japan). In addition, Zhou et al. [71] employed an ensemble neural network to predict the contact fatigue life of the AT40 coating. Neural networks are currently the mainstream method in the data-driven area, and their strong nonlinear function approximation capabilities offer robust support for better prediction. Figure 9 shows a general procedure for predicting gear contact fatigue via the back propagation (BP) neural network, which comprises an input layer, a hidden layer, and an output layer. The weight and bias parameters in such a neural network are trained using the BP algorithm.

Random forest (RF) is a widely accepted method for contribution analysis, and the mean decrease accuracy (MDA) algorithm is often used to analyze the importance of various surface integrity factors [72]. The variable importance measure (VIM) can be expressed as Eq. (10):

$$\mathrm{VIM}(X) = \frac{1}{N_\mathrm{T}} \sum_{j=1}^{N} \left(\mathrm{ER}_j - \mathrm{ER}_j'\right) \tag{10}$$

where N_T is the number of trees in the RF; ER_j is the prediction error of tree j before the disturbance of the characteristic variable X; ER_j' is the prediction error of tree j after the disturbance of the characteristic variable.

Numerous alternative algorithms, such as CatBoost [73], principal component analysis (PCA) [74], gray relational analysis (GRA) [75], and fuzzy comprehensive evaluation (FCE) [76], are also commonly used in contribution analysis. CatBoost is constructed based on gradient-boosting decision trees and is suitable for handling datasets with categorical features. PCA transforms multiple correlated variables into a few uncorrelated principal components through linear transformation, identifying the main influencing factors. The GRA evaluates the importance of each factor by calculating the gray relational degree between each factor and the reference sequence. FCE uses the principles of

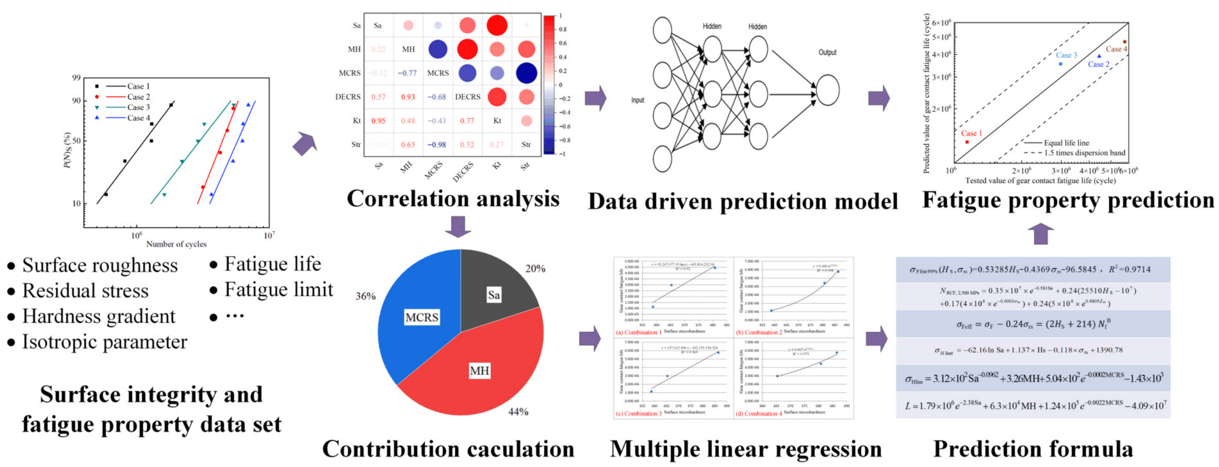

Fig. 8 A data-driven outline for predicting gear fatigue considering surface integrity.

fuzzy mathematics to assess multiple factors comprehensively, determining the importance of each factor.

(3) A data-driven case study

Table 1 lists some experimental data concerning the contact fatigue of carburized gears [77]. The surface roughness (*Sa*), the surface hardness (MH), the maximum compressive residual stress (MCRS), the depth of effective compressive residual stress (DECRS), the stress concentration factor (*Kt*), and the surface isotropic parameter (*Str*) are chosen as initial input parameters on the basis of prior experience. The output parameter is the contact fatigue life *L* under a given loading condition.

The correlation coefficients between the six parameters are obtained via the Pearson method. The absolute values of the correlation coefficients between *Sa* and *Kt*, MH and DECRS, MCRS and *Str*, exceed 0.9. By excluding *Kt*, DECRS, and *Str* and considering *Sa*, MH, and MCRS as the three retained surface integrity parameters, their contributions to the gear contact fatigue life are 40%, 37%, and 23%, respectively. Three cases (cases I, III, and IV) were chosen to curve-fit the relationships between each parameter and the fatigue life. Combining their contributions, Eq. (11) for predicting gear contact fatigue life at a constant loading (2,200 MPa) was formed.

$$L = 1.79 \times 10^6 \times e^{-2.38Sa} + 6.3 \times 10^4 \mathrm{MH} + 1.24 \times 10^5 \times e^{-0.0022\mathrm{MCRS}} - 4.09 \times 10^7 \quad (11)$$

Using case II as an example, the predicted and tested lives agree well, with a difference of only 13.11%. As shown in Fig. 10, the predicted fatigue lives of the four cases are within 1.5 times the dispersion band, an acceptable level in engineering practice [78], providing a quick guideline for gear anti-fatigue design.

In addition to establishing a prediction formula for gear contact fatigue life, a gear contact fatigue limit prediction equation (Eq. (12)) is also developed and corrected [77, 79].

$$\sigma_{\mathrm{Hlim}} = 14.2 \times e^{0.0016\mathrm{MCRS}} - 3.9 \times Sa^{2.1} - 6.4 \times 10^2 \times e^{-0.0045\mathrm{SRCS}} - 2.3 \times 10^7 \times e^{-0.018\mathrm{SH}} + 1830.2 \quad (12)$$

where MCRS is the maximum compressive residual stress, SCRS is the surface compressive residual stress, and SH is the surface hardness.

Figure 11 shows the relative errors between the test values and the predicted values of the gear contact fatigue limits. The maximum relative error is less than 5%, with an average error of 2.9%, which is satisfactory for engineering applications.

These encapsulate a variety of models for gear contact fatigue and delineate their respective advantages and disadvantages in Table 2.

4 Gear contact fatigue tests

The gear fatigue test is the most straightforward and efficient way to evaluate fatigue performance. Many institutions have pioneered test rig development, test method compilation, fatigue database construction, and test specification development. It is necessary to enhance gear fatigue testing as new gear geometries, new material compositions, new lubrication conditions, and new manufacturing processing technologies continue to advance.

4.1 Gear contact fatigue test rigs

In the mid-20th century, the Gear Research Center (FZG) at the Technical University of Munich manufactured the first series of power circulating gear back-to-back test rigs with a maximum loading capacity of 1,800 MPa [80]. The rig is widely used today

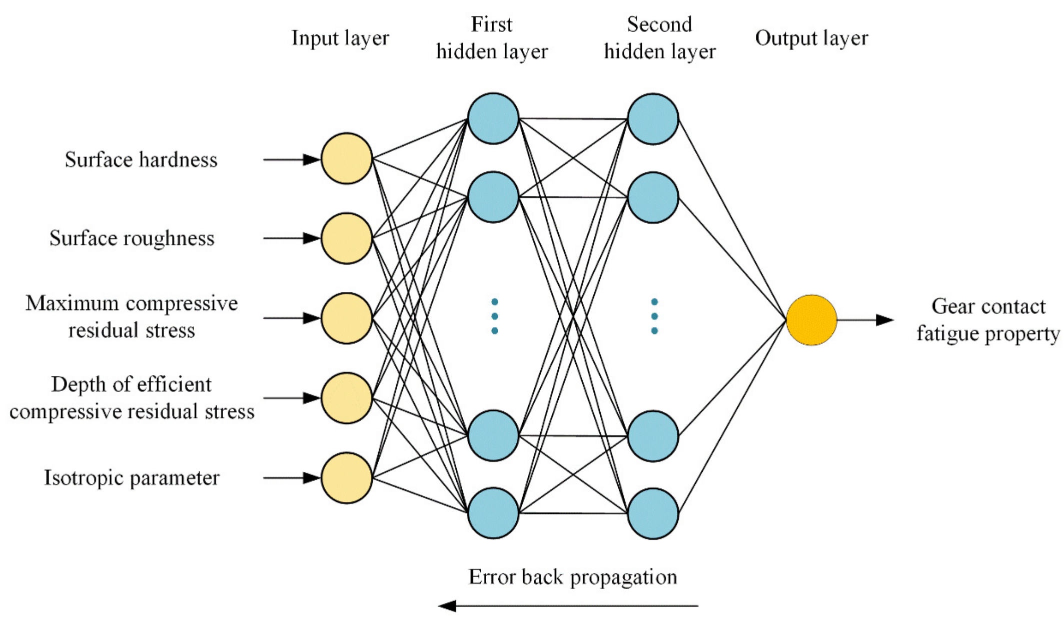

Fig. 9 Gear contact fatigue prediction via a BP neural network.

Table 1 Experimental data on contact fatigue lives of carburized gears [77]

	Sa (μm)	MH (HV)	MCRS (MPa)	DECRS (μm)	*Kt*	*Str*	*L*
Case I	0.75	658.7	−550.67	0	1.82	0.04	1.14×10^6
Case II	1.60	680.8	−1,236.00	123	2.47	0.86	4.43×10^6
Case III	0.23	665.3	−1,131.56	5	1.74	0.93	2.98×10^6
Case IV	0.36	686.5	−1,161.89	99	1.86	0.82	5.76×10^6

for testing transmission efficiency, surface scuffing, contact fatigue, and bending fatigue. In the 1970s, the National Aeronautics and Space Administration (NASA) produced a gear fatigue test rig for high-speed and heavy-duty conditions with a maximum rotational speed of 10,000 r/min [81]. The Strama-MPS corporation recently developed a high-speed FZG back-to-back test rig with a maximum speed of 18,000 r/min [82]. The design unit (DU) at Newcastle University developed a gear fatigue test rig that focuses on an increased center distance and a large tooth module, with a maximum torque of up to 6,000 N·m [83]. These test rigs are utilized to test a variety of materials, manufacturing processes, gear sizes, and lubrication conditions. The classifications of the gear test rigs are shown in Fig. 12. They can be classified into power opening and power circulating types depending on the manner in which the power is transmitted. Furthermore, these test objects can be further classified into

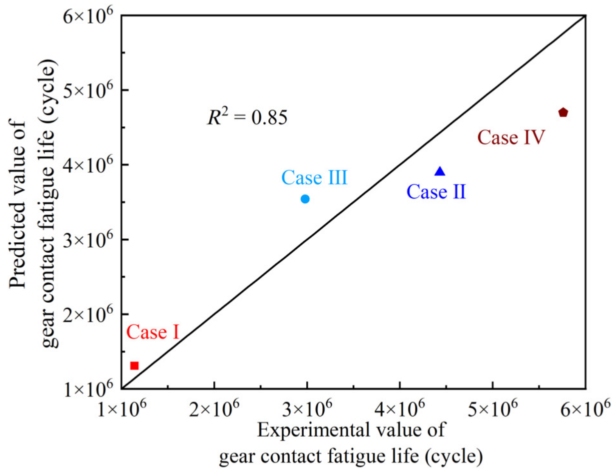

Fig. 10 Comparison of predicted and tested lives. Reproduced with permission from Ref. [77], © Elsevier Ltd. 2022.

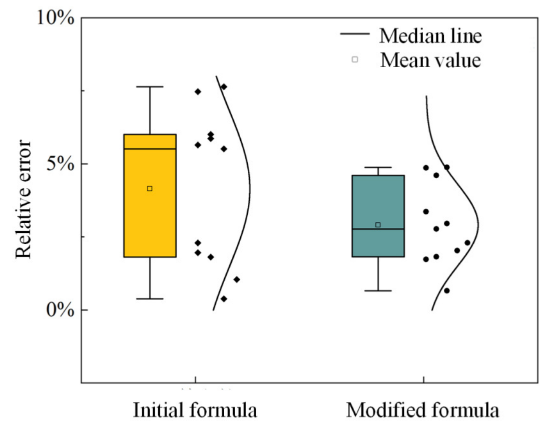

Fig. 11 Prediction errors of gear contact fatigue limit. Reproduced with permission from Ref. [79], © Editorial Office of the Chinese Journal of Mechanics 2024.

Table 2 Advantages and disadvantages of gear contact fatigue methods

Type	Model	Advantage	Disadvantage
Statistical model for gear contact fatigue life	L–P [30, 31]	By applying the principle of material failure and accounting for the effects of maximum stress on stress volume, this approach exhibits broad applicability for research purposes.	Based on the assumption of a smooth surface and subsurface fatigue crack initiation, while neglecting the effects of tangential stress, the determination of multiple parameters requires experimental investigation.
	I–H [33]	By considering the integration of stress magnitudes and their corresponding depth distribution throughout the stress volume, a more accurate and comprehensive methodology is obtained.	Gear fatigue failure is thought to occur only when the stress level surpasses the fatigue limit, leading to an overestimation of the fatigue life.
	Zaretsky [34]	It is a general method for predicting the fatigue life of structural components, which can be achieved by using finite element analysis.	The relevant parameters need to be obtained empirically, and factors such as material inhomogeneity and residual stress are ignored.
Deterministic model for gear contact fatigue life	B–M [48, 51]	It can predict the most realistic fatigue life of ductile metals and is the preferred fatigue criterion for conventional materials at room temperature.	Without considering the effect of mean stress, it cannot reflect the effect of initial residual stress.
	F–S [49, 52]	Considering the effects of nonproportional loading-induced strengthening and residual stress on multiaxial fatigue damage	The prediction of most crack orientations is not very accurate.
	D–V [50]	Emphasis is placed on the effects of time-varying stress history and high-amplitude hydrostatic stress.	Excessive conservatism of the calculated risk of failure can occur if the hydrostatic stress value of a material point is excessively high.
Prediction model for gear contact fatigue strength	ISO [18]	Taking into account comprehensive factors and incorporating numerous correction coefficients, the results are relatively accurate.	The complexity of the formula leads to a protracted computational time. Additionally, the calculated results are relatively conservative.
	AGMA [58]	Providing graphs and charts for most of the coefficients enables easy and rapid computations.	There are a few factors taken into consideration, resulting in coarse calculations.
Data-driven model for gear contact fatigue	Correlation analysis & data-driven.	It is unnecessary to have a comprehensive understanding of the exact mechanism behind its failure, as it exhibits remarkable self-learning capability and can make precise predictions.	It is essentially a black-box model that cannot provide quantitative equations.
	Correlation analysis & contribution analysis & formula fitting [77, 79]	This approach is capable of elucidating the importance of every parameter and making quantitative predictions about the gear contact fatigue property.	The prediction accuracy depends on both the selected parameters and the available data quantity.

equivalent fatigue test rigs, normal fatigue test rigs, and special fatigue test rigs.

The gear contact fatigue test is costly and time-consuming. To address data shortages and testing challenges, researchers have proposed the use of rolling–sliding contact fatigue tests (equivalent contact fatigue tests) with the same radius of curvature as gears for simulation [84]. The roller samples replicate gear pitch line contact, with the disk roller's equivalent curvature radius being crucial in design [84]. This method effectively assesses gear tribological properties [85, 86] and fatigue crack characteristics [87]. In the mid-20th century, NASA designed a five-ball fatigue test rig to explore the effects of residual stress, lubricants, and hardness on fatigue life. Various types of test rigs with distinct principles suitable for different contact forms and operating conditions, such as roller test rigs and ball–disc test rigs, have since been developed. One of the most iconic test rigs among them is the roller fatigue test rig initially established by Merritt [88]. Meneghetti et al. [89] developed a twin-disc test rig and reported that the most crucial parameters were the specimen radius and sliding speed. Ahlroos et al. [90] discovered that DLC coatings and grease lubrication notably enhance fatigue resistance when a twin-disc rig is used. Li et al. [91] proposed a transfer learning framework to predict gear contact fatigue life via roller fatigue data, with a prediction error of 46.33%, indicating the applicability of an equivalent contact fatigue test.

Considering factors such as standardization, universality, and reliability, most scholars utilize primarily medium-module cylindrical gears and normal gear test rigs to conduct gear contact fatigue tests. Figure 13 shows some typical normal gear fatigue test rigs that are used to test medium module cylindrical gears. Chongqing University has developed a power opening gear test rig with variable center distances [92], with a maximum speed of 4,500 r/min, maximum torque of 236 N·m, and tooth module range of 1–5 mm. The power opening type has certain drawbacks, such as large energy consumption and energy waste. Therefore, most current gear fatigue test rigs adopt a power circulation scheme. Test rigs developed by FZG, DU, and NASA are of the power circulating type. The FZG back-to-back test rig with a center distance of 91.5 mm allows tests at maximum torques of 600 N·m and rotational speeds in the range of 13–8,500 r/min under dip or spray lubrication. All damage types, including pitting, micropitting, wear, scuffing, tooth root bending, and tooth flank fracture, can be investigated by adequately defining the gear geometry and operating conditions. The FZG test rig is the foundation for many tests, such as the scuffing test in ISO 14635 [93], the micropitting test in DIN 3990-16 [65], the pitting test in CEC-L-108 [94], and the wear test in DGMK 377 [95]. In addition to test rigs with fixed center distances, Strama-MPS has designed a variable center distance (89–140 mm) gear test rig with a maximum speed of 6,000 r/min and a maximum torque of 2,100 N·m [96].

In addition to the normal gear fatigue test rigs used to test

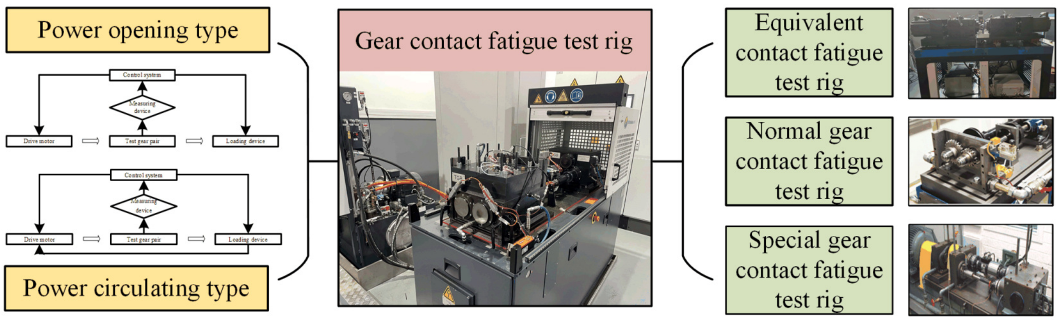

Fig. 12 Classifications of gear contact fatigue test rigs.

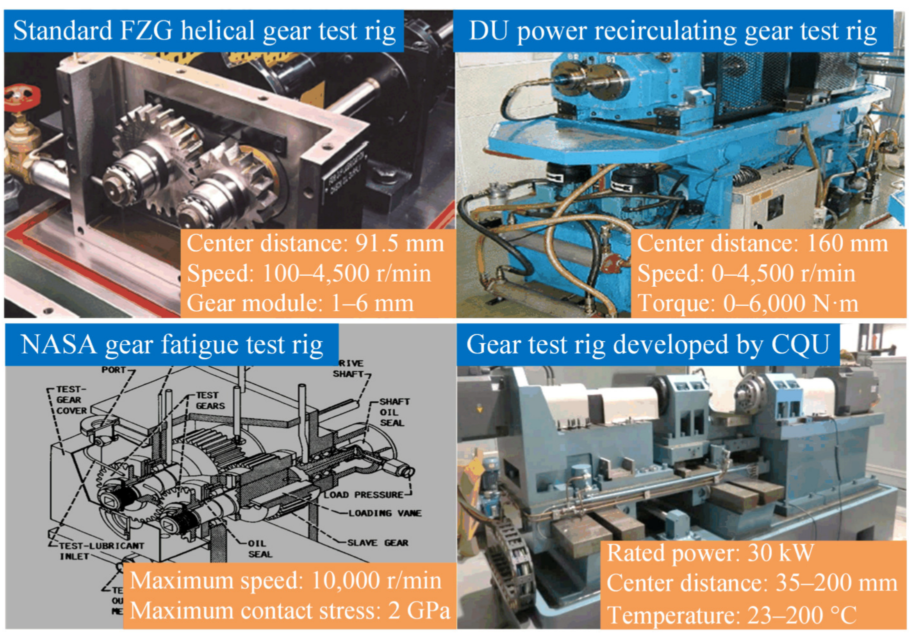

Fig. 13 Typical normal gear fatigue test rigs to test medium module cylindrical gears. Reproduced with permission from Ref. [97]; from Ref. [98], © the authors 2016; from Ref. [99], © Elsevier Ltd and Techna Group S.r.l. 2021.

medium module cylindrical gears, several special test rigs have been developed in recent years, as shown in Fig. 14. To investigate gears that are larger or smaller than the standardized gear with a module of 4.5 mm [93, 100], test rigs with center distances of 200 and 7.5–52 mm [101] are available. Certain test rigs are equipped with a hydrostatic torque application to realize load spectra during testing. For investigations at increased circumferential speeds, a high-speed test rig was developed [82]. The internal gear test rig [102] allows investigations on the load-carrying capacity of the meshing of the planet and ring gear (convex–concave pairing) in planetary gear stages. To test the bevel and face gears, the TS-30 bevel gear test rig developed by Strama and Klingelnberg, with a module of 1.5–5 mm, a gear ratio of 1–2.5, and a shaft interlaced angle of 60°–120°, enables the testing of the wear and fatigue strength of bevel gears [83]. In addition, Strama designed a hyperboloid gear test rig with a maximum speed of 6,000 r/min and a maximum torque of 3,000 N·m [103]. FZG has also developed a power circulating bevel and hypoid gear test rig (with shaft offset distance adjustment), with a maximum external diameter of 170 mm and speeds ranging from 100 to 4,800 r/min [104]. Special test rigs to investigate worm gear geometries are available that consider a wide range of gear center distances [105].

Monitoring of gear signals in service, including vibration, temperature, and stress, plays a pivotal role in assessing operating performance [106]. Sharp changes in vibration signals can occur due to failures such as pitting and cracks. Their monitoring typically involves the use of Fourier transforms, wavelet transforms, ensemble empirical mode decomposition, and higher-order spectra. Lu et al. [107] employed infrared sensors to identify temperature changes during plastic gear running, revealing a substantial increase in gear bulk temperature and a decrease in fatigue life as the torque increases or the oil supply shrinks. Various measuring technologies, such as strain gauges, grating detections, and photoelastic experiments, are employed to measure the stress and strain of gear teeth. The development of integrated measuring devices capable of handling multiple signals will be a major research focus in the future. As shown in Fig. 15, a wireless condition monitoring system that measures temperature, strain, and vibration was developed by Wei et al. [108]. Using the wireless condition monitoring system developed by Wei et al. [108], signals of stress, vibration, and temperature were measured during the testing process to assess operating performance. The results indicate that when gear failure occurs, there is a significant increase in temperature, vibration, and stress signals, demonstrating that precise detection of these signals can be used to assess the operational performance of gears effectively.

The authors have summarized some experience in gear contact fatigue testing. First, the gear shaft key slot may be deformed or even fractured due to excessive torque. To avoid this issue, the use of shaft materials with a hard surface and tough interior by carburizing or nitriding treatment is advised. Second, ensuring high reliability for sealing rings is important, as their failure could result in oil leakage and other related issues. Third, during tests, the mixture of iron chips in the lubricant is inevitable. This results in an overall decrease in the quality of the lubricating oil. As such, it is imperative to perform routine replacements of both the lubricating oil and the filter element to keep the oil clean. Fourth, maintaining the lubricating oil temperature within the range of 60–80 °C is advisable to prevent issues with reduced fluidity at low temperatures and degradation at high temperatures unless the operating temperature is explicitly determined. Fifth, some elements, such as bolts, nuts, and pins, are prone to wearing out after long-term operation, and sufficient spare parts should be prepared. Sixth, using the staggered installation scheme can effectively avoid bending fatigue failure during contact fatigue tests. Seventh, a low-load and low-speed running-in procedure conducted for 2–3 h can aid in achieving normal operation. Eighth, to mitigate the risk of excessive instantaneous impact, it is advisable to apply torque using a step-by-step loading method. Ninth, it is feasible to use peepholes to observe tooth surface conditions and optimize inspection intervals by analyzing failure conditions. This will increase the test efficiency. Tenth, the new generation of gear fatigue test rigs should be able to operate reliably under extreme working conditions such as ultrahigh-speed, ultrahigh-load, high- or low-temperature, and loss-of-lubrication conditions.

4.2 Gear contact fatigue test methods

Common test methods for assessing gear contact fatigue include the staircase test method, the group method, the few-sample test

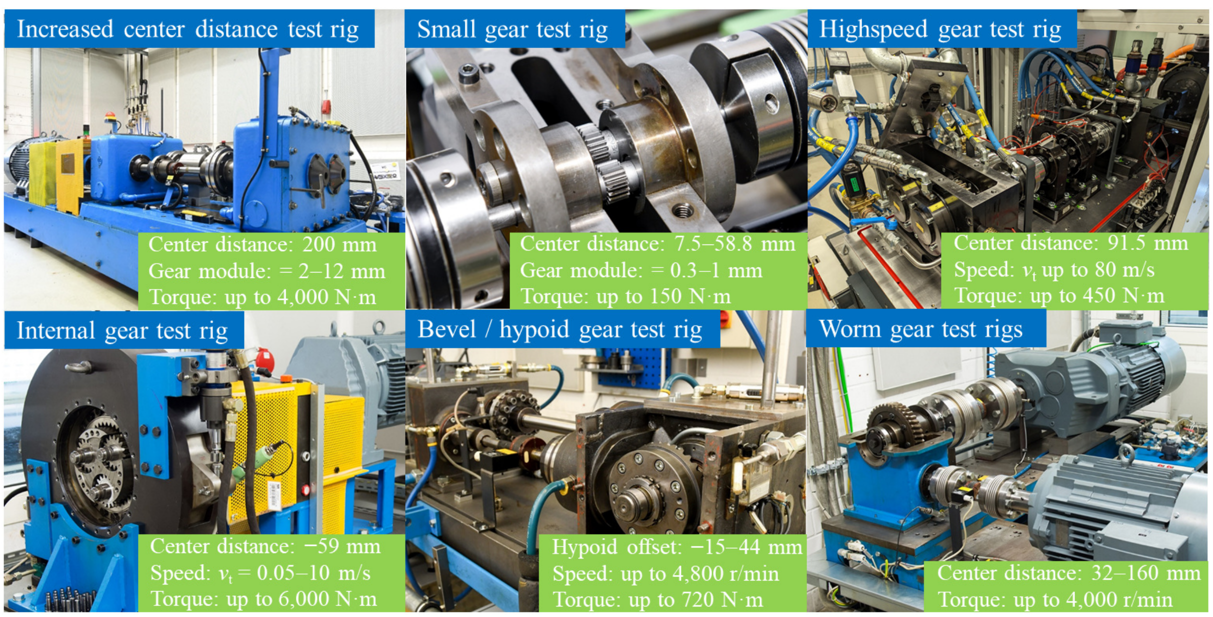

Fig. 14 Some special gear fatigue test rigs.

method, and the accelerated test method. Figure 16 shows some of the test methods. As shown in Fig. 16(a), the staircase test method [109] employs 4–7 loading stages, in which at least 20 effective test points in total are needed. It is capable of determining the gear fatigue limit, but generally speaking, it is time- and cost-consuming. Different accelerated test methods have emerged to address this issue. The Locati method [110] is among the most popular methods. As shown in Fig. 16(b), the Locati method utilizes a step-by-step loading test on a single gear pair until contact failure occurs. The gear fatigue limit is then calculated according to the Miner damage accumulation criterion. Empirical evidence indicates that its accuracy is heavily contingent on the initial estimation of the fatigue limit. The number of loading stages is typically in the range of 10–16, and the critical loading stage when the gear fails should be no less than 6. The cycle ratio, defined as the ratio between the stress interval and the number of cycles of each loading stage, usually falls into the range of $(1–2.5)\times10^{-4}$ MPa. Compared with the staircase method, the

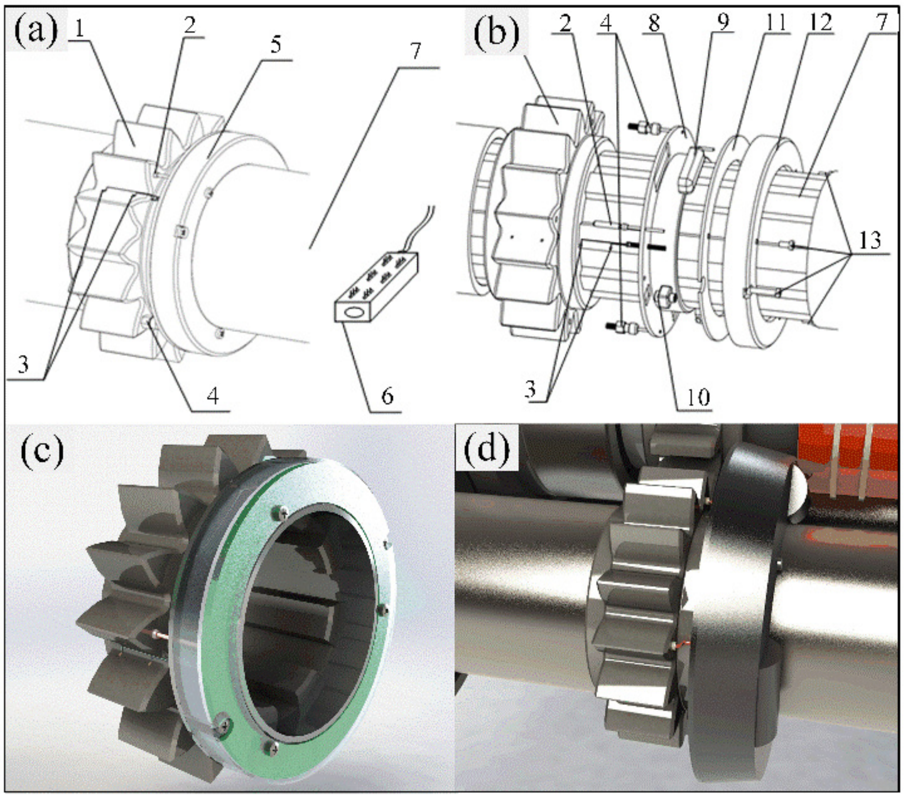

Fig. 15 Gear wireless condition monitoring system: (a) 3D model, (b) installation diagram, (c) measuring device, and (d) installation on gear systems. Reproduced with permission from Ref. [108] for (a, b), © 2022.

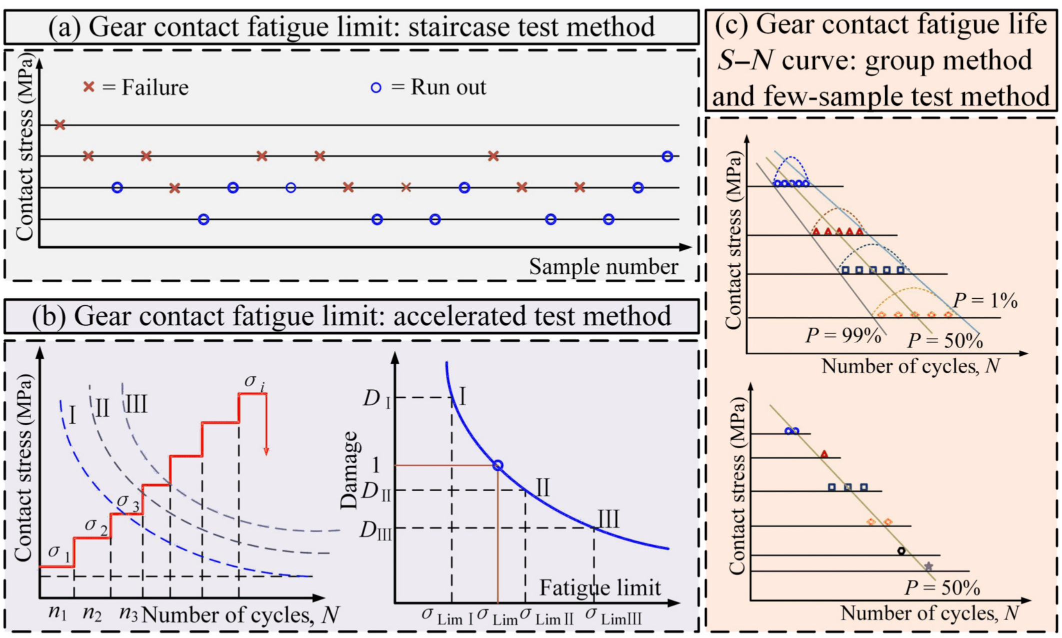

Fig. 16 Test methods for gear contact fatigue.

Locati method reduces the testing cost by at least 60% without significant differences in the results. The Probit method [111] can also be applied to determine the gear fatigue limit. Typically, tests are conducted at 4–5 loading stages, with the failure probability at each loading stage being statistically analyzed. Through linear regression, fatigue limits with different reliabilities are obtained.

The *S*–*N* curve can be determined via the group method and the few-sample test method [112]. The group method involves four or five loading stages. There are generally five repeated test points at each loading stage, as shown in Fig. 16(c). The few-sample test method is a rapid method for determining the *S*–*N* curve. The method conducts a small number of tests at multiple loading stages, with no fewer than 7 points in total. However, it is only applicable to the *S*–*N* curve with 50% reliability, as shown in Fig. 16(c). However, in current engineering practice, engineers prefer to use a much higher reliability, e.g., 99% reliability. For the group method, the minimum loading stage can be determined as 1–1.05 times the estimated fatigue limit, whereas the maximum loading stage can be determined as 1.3–1.4 times the fatigue limit.

The selection of the test method should consider actual circumstances. When sufficient samples and time or high-precision results are available, the staircase test method and the group method are recommended for the fatigue limit and *S*–*N* curve, respectively. When the sample number is small or people do not have the patience to wait a long time, accelerated methods such as Locati and the few-sample test method are recommended for the fatigue limit and *S*–*N* curve, respectively. The loading of the aforementioned test methods is constant. However, under real operating conditions, gears usually experience a wide spectrum of loads. Therefore, gear fatigue test methodologies under variable load spectra should be explored. Hein et al. [113] proposed a test methodology for gear time-scaled fatigue tests on the basis of a variable load spectrum. Chen [114] developed a gear load spectrum and an accelerated fatigue test method for aircraft engine accessory gearboxes based on the principle of damage equivalence. These advancements in test methods have supported the accurate estimation of gear life in various fields, such as wind turbines, automobiles, and aviation machines.

4.3 Gear contact fatigue data processing

Data processing methods have been developed for gear fatigue estimation. To derive the *S*–*N* curve, the group method and the few-sample test method are used. The data processing method primarily consists of four steps:

Step 1: ranking of test points by fatigue life

Under a loading stage, the total number of test points is denoted as n, and the ranking of their fatigue lives is as Eq. (13):

$$N_{\mathrm{L}1} \leqslant N_{\mathrm{L}2} \cdots \leqslant N_{\mathrm{L}n-1} \leqslant N_{\mathrm{L}n} \tag{13}$$

The median rank formula of the life distribution function of any fatigue life $N_{\mathrm{L}i}$ is given by Eq. (14):

$$P(N_{\mathrm{L}i}) = \frac{i-0.3}{n+0.4} \tag{14}$$

where n is the total number of test points and i is the serial number of tests for the fatigue life, ranked from low to high.

Step 2: assumption of distribution

According to many investigations [115, 116], the gear fatigue life typically follows normal, lognormal, or Weibull distributions. Equations (15)–(17) represent the logarithmic forms of the three distributions

$$\phi^{-1}(P(N_{\mathrm{L}})) = \frac{1}{\sigma_{\mathrm{N}}}(N_{\mathrm{L}} - \mu_{\mathrm{N}}) \tag{15}$$

$$\phi^{-1}(P(N_{\mathrm{L}})) = \frac{1}{\sigma_{\mathrm{lnN}}}\ln(N_{\mathrm{L}} - \mu_{\mathrm{lnN}}) \tag{16}$$

$$\ln\ln\frac{1}{1-P(N_{\mathrm{L}})} = \beta\left(\ln(N_{\mathrm{L}} - \gamma) - \ln\eta\right) \tag{17}$$

where N_{L} is the gear fatigue life; μ_{N} is the mean value of the normally distributed population; σ_{N} is the standard deviation of the normally distributed population; similarly, μ_{lnN} is the mean value of the lognormally distributed population; σ_{lnN} is the standard deviation of the lognormally distributed population; β is the shape parameter of the Weibull distribution; η is the scale parameter; γ is the location parameter.

Step 3: determination of the distribution function

$P(N_{\mathrm{L}i})$ is calculated via Eq. (14), and distribution function fitting is performed via Eqs. (15)–(17). To select among the three life distributions, the least squares method should be employed for goodness-of-fit testing. When the minimum linear correlation coefficient satisfies two or more distributions, a distribution with a larger absolute value of the linear correlation coefficient should be preferred.

Step 4: determination of the *S*–*N* curve

By utilizing the life distribution function, the calculated life at a specified reliability R, $N_{\mathrm{L},R}$, can be determined. According to the different loading stages, the calculated lives are used to fit the *S*–*N* curve. The fitting formula is as Eq. (18) [117]:

$$\sigma_{\mathrm{H}}^{m} N_{\mathrm{L},R} = C \tag{18}$$

For the staircase test method, the data processing method consists of three steps.

Step 1: statistical analysis of the test points and stress rankings

"Run-out" or "failure" is selected as the "analytical event" on the basis of the principle of fewer total points. The loading stages are ranked in ascending order, with l representing the loading stage number, as given by Eq. (19).

$$\sigma_0 \leqslant \sigma_1 \leqslant \cdots \leqslant \sigma_l \tag{19}$$

Step 2: calculation of the mean stress and standard deviation.

Equations (20) and (21) are used to calculate the mean stress and standard deviation:

$$\mu_{\sigma} = \sigma_0 + \Delta\sigma\left(\frac{A}{N} \pm \frac{1}{2}\right) \tag{20}$$

$$s_{\sigma} = \begin{cases} 1.6\Delta\sigma\left(\dfrac{NB-A^2}{N^2} + 0.029\right), & \dfrac{NB-A^2}{N^2} \geqslant 0.3 \\ 0.53\Delta\sigma, & \dfrac{NB-A^2}{N^2} \leqslant 0.3 \end{cases} \tag{21}$$

where "−" represents "failure"; "+" represents "run out"; $\Delta\sigma$ is the stress interval.

The values of A, B, and N can be found in the Chinese standard GB/T 14229-2021, as given by Eq. (22).

$$\begin{cases} A = \sum\limits_{i=0}^{l} i f_i \\ B = \sum\limits_{i=0}^{l} i^2 f_i \\ N = \sum\limits_{i=0}^{l} f_i \end{cases} \tag{22}$$

where f_i is the number of occurrences of each loading stage within the analytical event.

Step 3: determination of the fatigue limit.

The fatigue limit under various reliabilities R can be calculated as Eq. (14) [118]:

$$\sigma_R = \mu_\sigma + \Phi^{-1}(1-R)\Delta\sigma s_\sigma \tag{23}$$

While many data processing methods have been proposed, most require a relatively large number of test points. To address this limitation, the authors focused on data enhancement and data transfer methods [119–121]. For example, Mao et al. [122] proposed an S–N curve fitting model based on the hierarchical Bayesian method, which was suitable for few-sample conditions. The model incorporates additional information concerning the fatigue life distribution beyond the stress level. Those experimental findings demonstrate that the model is superior to traditional least squares methods. Mao et al. [123] proposed a statistical method for determining the gear fatigue limit on the basis of Monte Carlo sample expansion and standard deviation correction, which ensures high accuracy even when the sample size is reduced by 40%. Lu et al. [124] presented a predictive model for the contact fatigue life of PEEK gears via CTAB-GAN data augmentation. These results revealed that the predicted fatigue lives based on the enhanced dataset are within a twofold scatter band. These data processing methods have been incorporated into gear design software, which is convenient for engineering practice.

4.4 Gear fatigue database

The experimental database is a crucial prerequisite for high-performance gear design, as it provides direct data for assessing gear fatigue life and failure modes. Institutions such as FZG, ASME, and NASA, to name a few, have developed high-reliability test rigs and constructed durability databases to support gearbox design. FZG has accumulated a substantial amount of experimental data via self-developed test procedures, providing the foundation for series gear design specifications such as ISO 6336 and DIN 3900. ASME has conducted approximately 3,000 tests on the fatigue properties of various material gears over 15 years, with results incorporated into the AGMA 2104 specifications. Since the 1970s, the NASA Lewis Research Center has undertaken approximately 1,000 gear contact fatigue tests utilizing their 10,000 r/min test rig, covering nearly 20 types of materials, including 4,620, 9,310, and M50, and manufacturing processes such as carburizing, nitriding, shot peening, finishing, and coating. The test work at NASA then supported gear transmission design for the U.S. aerospace industry [89]. Chongqing University also conducted a series of gear fatigue tests involving various materials, such as 16Cr3NiWMoVNbE, 9310, 8620H, 20CrMnTi, and 18CrNiMo7-6, with manufacturing processes such as grinding, nitriding, shot peening, coating, and barrel finishing. On the basis of these data, empirical formulae for gear fatigue assessment have been proposed [77, 79].

5 Influential factors of gear contact fatigue

The gear contact fatigue failure mechanism is complicated because it is affected by various factors, as shown in Fig. 17, including structural factors such as gear geometry and surface morphology; working conditions such as torque and speed; and material factors such as yield strength and residual stress. Although some important factors have been identified, further studies are still being conducted to understand more influential factors and their interactions.

5.1 Influences of operating conditions on gear contact fatigue

Operating condition factors include torque, speed, temperature, and lubrication. Gears typically endure a nonconstant torque history, so it is necessary to consider the effect of the load spectrum on gear contact fatigue in addition to the inverse relationship between the load and fatigue life (known as the S–N curve). Liu et al. [125] proposed a gear contact fatigue model that considers the load spectrum via the rain-flow counting method. They reported that the contact fatigue life increases by 1.92 times compared with that of the reference constant load condition because of the contribution of a series of low-level load stages. The maximum damage depth is deeper because of the roles of a series of high-load levels. The rotational speed affects the local contact area and frictional characteristics of the tooth surface, thereby affecting contact fatigue [126]. Olver [127] reported that torque and speed are the main factors influencing lubrication conditions and operating temperature. This occurred because a higher load and speed can increase the temperature and decrease the film thickness. The lubrication condition is primarily determined by the film thickness, which can be influenced by both the amount of lubrication and the lubrication type. Moss et al. [128] experimentally reported that gears with high-speed jet lubrication (J1, J2) have a longer fatigue life than those with dip lubrication (D1), as shown in Fig. 18. Lubricants also influence the gear contact fatigue. Winter and Knauer [129] performed systematic investigations on the influence of lubricant and operating

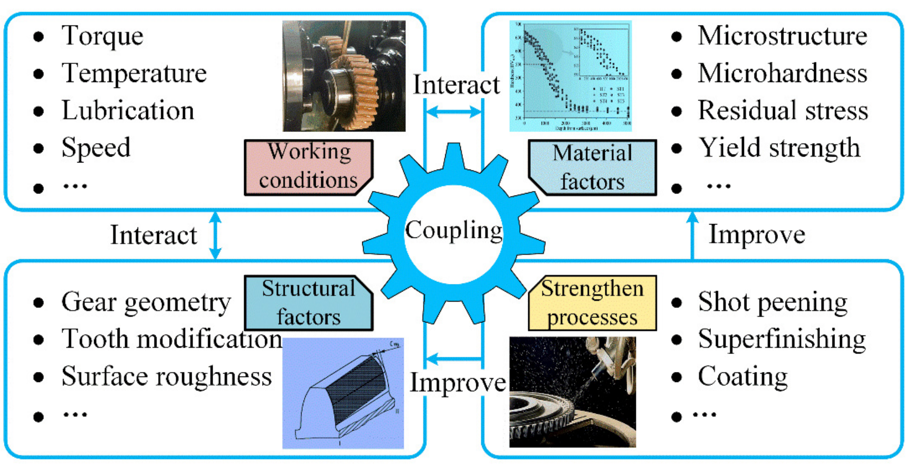

Fig. 17 Factors of structure, material, and working conditions that influence gear contact fatigue.

temperature on the pitting load-carrying capacity of case-hardened gears. Notably, a standardized pitting test according to CEC-L-108 [130] allows a rating of lubricant performance and an investigation of the influence of different lubricant properties, including those of oil additives. Further influencing factors of the lubricant on gear contact fatigue were investigated. Newly developed water-based lubricants [131, 132] for high-speed applications, such as BEV gearboxes, have been investigated to reduce frictional coefficients and increase mechanical efficiency. The gear operation temperature is influenced by various factors, including torque, speed, and lubrication. High temperatures can cause a decrease in lubrication viscosity, rupture of the oil film, and an increase in the frictional coefficient, potentially resulting in tooth surface wear, scuffing, and material phase transformation or even softening. Ensuring comprehensive control over the torque, speed, and lubrication is an indispensable approach to enhancing gear contact fatigue resistance.

5.2 Influences of structural factors on gear contact fatigue

The main gear structural factors include gear geometry, tooth modification, and surface roughness. The gear geometry parameters include the tooth module, pressure angle, and addendum factor. When the tooth module increases, the risk of bending fatigue failure generally decreases, but this results in a decrease in the number of teeth, thus increasing the risk of contact fatigue failure. A small pressure angle increases the stress concentration on the tooth surface, which can lead to pitting, although it can also confine the high-stress region to the hardening layer, thereby reducing gear tooth internal damage. Consequently, pressure angle design must be considered from various perspectives. A high contact ratio can be achieved in different ways, namely, by lowering the pressure angle and increasing the addendum factor, ultimately reducing the contact stress, as shown in Fig. 19(a) [133]. Tooth modification is often employed to alleviate uneven loading of tooth surfaces. Guilbault and Lalonde [134] utilized particle swarm and firefly algorithms to determine tip relief, which significantly enhances anti-fatigue properties. Qin and Guan [135] analyzed the contact stress distribution before and after tooth profile modification and concluded that appropriate tooth profile modification helps prolong the fatigue life, as shown in Fig. 19(b). In addition, gear contact fatigue can also be affected by the helix angle, sliding condition, and material size. The investigations by Geitner et al. [136] focused on the pitting load capacity of internal spur gears and helical gears and recommended an extended contact analysis, such as that described in Ref. [137]. Further research has investigated the influence of different sliding conditions/orientations on the flank load-carrying capacity of internal gears [138]. An increased risk for pitting and micropitting formation is typically found in the flank areas of negative specific sliding. The investigations by Dobler et al. [101] revealed that the material volume/size influences the load-carrying capacity of very small module gears. Rough tooth surfaces create stress concentrations that result in issues such as pitting and micropitting, and affect material microstructure evolution and lubrication states on tooth surfaces. Ichimaru et al. [139] reported that interactions among rough peaks on tooth surfaces are the decisive factor influencing pitting. Zhang et al. [140] established an elastic–plastic finite element model to explore the effect of surface roughness on gear contact fatigue life. They reported that when the surface roughness increased from 0 to 1.1 μm, the contact fatigue life decreased from 10^7 to $10^{5.4}$, as shown in Fig. 19(c).

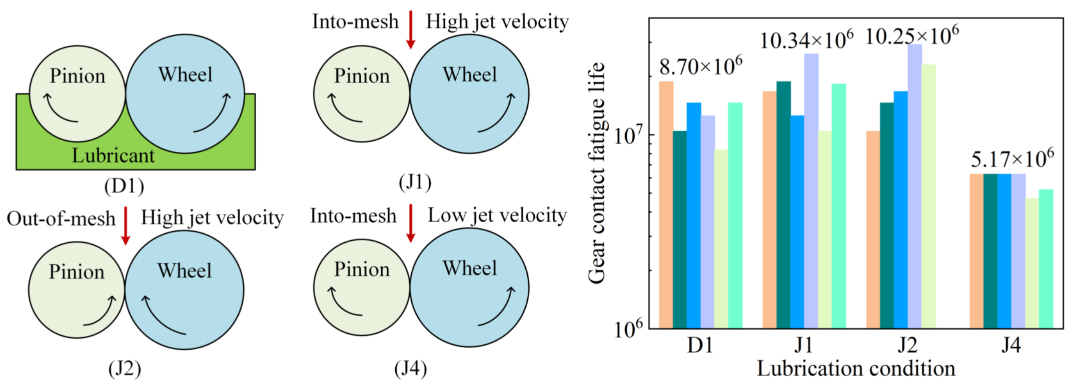

Fig. 18 Effect of lubrication type on gear contact fatigue. Reproduced with permission from Ref. [128], © ASME 2018.

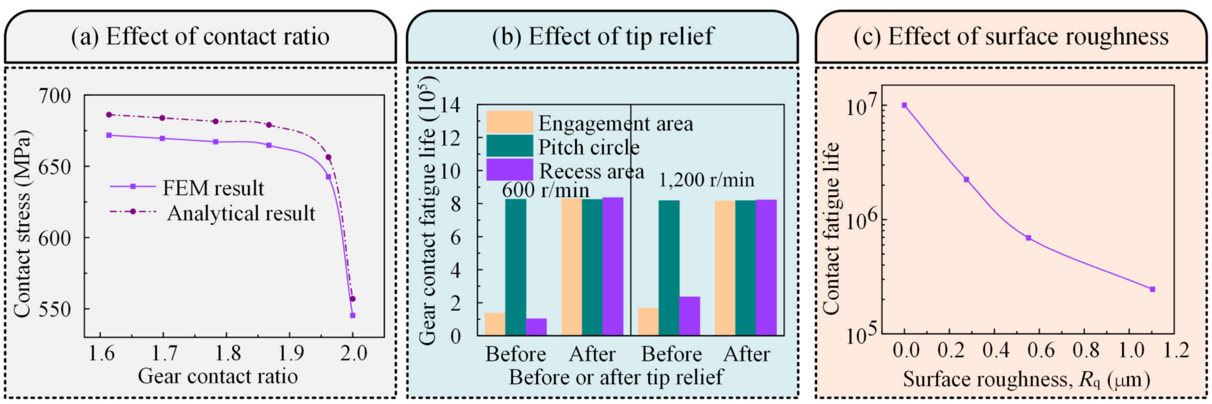

Fig. 19 Effects of structural factors on gear contact fatigue performance [140]. Reproduced with permission from Ref. [133] for (a), © INPRESSCO 2018; from Ref. [135] for (b), © Elsevier Ltd. 2014.

5.3 Influences of material factors on gear contact fatigue

After the gear structure and operating conditions are determined, its service performance primarily depends on the material factors. Klein [141] conducted gear contact fatigue tests with different materials and surface treatments and reported that, compared with AISI 8620 hobbing gears, AISI 4620M ground gears exhibited superior contact fatigue durability. Zhou et al. [142] discovered that isotropic materials have a greater contact fatigue life than anisotropic materials. Furthermore, the influence of microstructural material properties, such as cleanliness and grain size, was investigated by Fuchs et al. [143] and Rommel et al. [144]. Investigations for the optimization of contact fatigue performance by alloy modification can be found in Ref. [145]. The residual austenite content can be a critical indicator of the material properties of case-hardened gears. The experimental studies conducted by Zhu et al. [146] revealed that the key factors contributing to improved contact fatigue resistance are Austenite precipitates, Martensite, and austenitic toughness, as shown in Fig. 20(a). Roy et al. [147] investigated the effects of different residual austenite contents on the gear micropitting life, and the results indicated that a higher content of residual austenite should be ensured during gear heat treatment, as shown in Fig. 20(b). Güntner et al. [148] and Blech et al. [149] investigated the influence of alternative microstructures (e.g., near-surface precipitation conditions) on the contact fatigue resistance, revealing the high contact fatigue resistance potential of carbon nitrided gears with increased retained austenite contents. Liu et al.

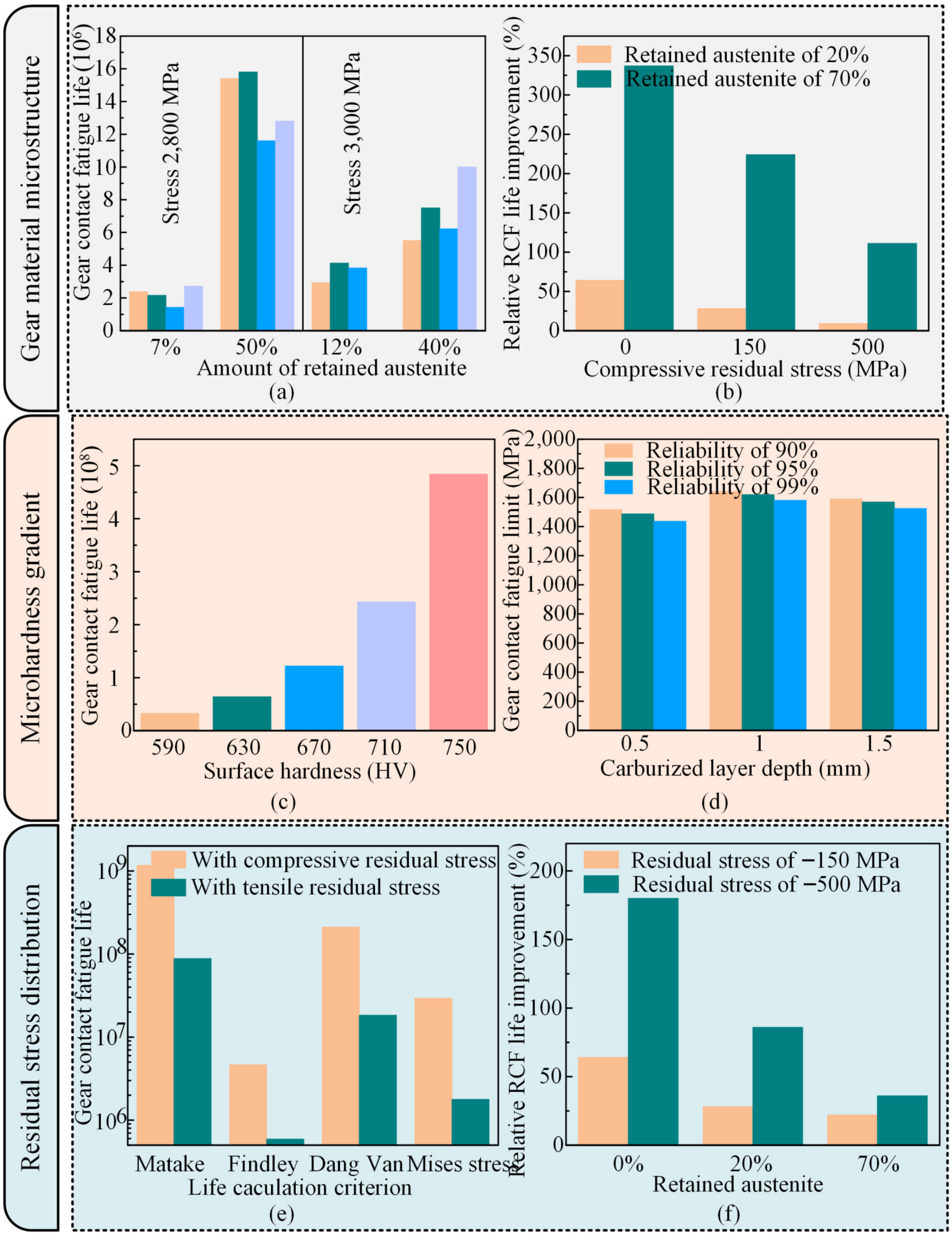

Fig. 20 Effects of material factors on gear contact fatigue performance [27, 40, 146, 147, 150–152].

[40, 150] reported that increases in surface hardness and hardness depth lead to a decreased risk of pitting and deep spalling failure, as shown in Fig. 20(c). According to the experimental study by Li et al. [151], the gear contact fatigue limit increases with increasing hardened depth, as shown in Fig. 20(d). The gear contact fatigue life can be improved by compressive residual stress, whereas tensile residual stress can increase the likelihood of contact fatigue failure [27, 152], as shown in Figs. 20(e) and 20(f). Ooi et al. [153] chose samples to conduct rolling contact fatigue (RCF) tests with different residual stress levels achieved by carburizing and tempering. The results showed that when the compressive residual stress (CRS) increased from −155.4 to −479.6 MPa, the observed RCF life was as much as 20 times the attainable life of the initial sample. Extended investigations [154] also revealed a significant reduction in the contact fatigue resistance of case-hardened gears with grinding burns due to near-surface microstructural and residual stress modifications.

Plastic gears are increasingly used because of their advantages, including light weight, low noise, and low cost. With the continuous advancement of material science and molding technology, plastic gears have garnered considerable attention. With the continuous study of plastic gears, high-strength plastic gears are increasingly being applied in various power transmissions, such as automotive engines, main drives of light vehicles, accessory gearboxes of aircraft engines, and wind power yaw pitch gearboxes. Lu et al. [155, 156, 158] and Yu et al. [157] conducted a continuous study for five years on the theory, experiments, and application of POM, PEEK, POK, and composite material gears under dry, oil, and grease lubrication conditions. More than 250 sets of plastic gear data were obtained, thereby promoting the development of the gear industry toward "replacing steel with plastics". Systematic investigations on plastic gears from different material pairings were performed, and adequate calculation methods were developed by Stahl and colleagues [159–162]. In particular, the work of Reitschuster et al. [163] highlights the potential of the use of high-performance plastic gears within automotive electromobility applications.

5.4 Influences of manufacturing processes on gear contact fatigue

Figure 21 shows several manufacturing processes to improve surface integrity and gear contact fatigue performance, including carburizing, nitriding, shot peening, rolling treatment, laser shock peening, surface finishing, particle peening, and thermal barrier coating. The commonly used heat treatment techniques, such as case-hardening (especially case-carburizing), nitriding, and surface hardening (e.g., induction hardening), can generate high hardness of the tooth surface layer while retaining sufficient plasticity and toughness in the core area [164–168]. Shot peening is a surface treatment technique in which high-speed shots are applied to the material surface to induce plastic deformation and refine the microstructure, resulting in improved fatigue strength. The contact fatigue performance of shot-peened gears is related primarily to the shot peening intensity and coverage, which should be reasonably determined considering the selected gear material and working conditions [169–173]. Li and Liu [174] reported that as the tooth surface hardness increases to 61.5–63 HRC by shot peening from the ground state of carburized gears, the gear contact fatigue limit increases by approximately 14.6%. A study conducted by Townsend [175] revealed that the fatigue life of high-intensity shot peening gears is 2.15 times greater than that of medium-intensity shot peening gears, with a contact stress of 1.71 GPa. According to Liu et al. [176], the crack initiation life of high-intensity shot peening samples was observed to increase under lower loads than that of low-intensity samples. However, this trend was reversed when the load exceeded a certain threshold. Conventional shot peening is subject to limitations where increased surface roughness potentially leads to reduced fatigue strength. As an emerging technology, FPP produces high compressive residual stress while reducing surface roughness, thereby significantly improving fatigue resistance. Moreover, laser shot peening, a technique involving high-power lasers and material interactions, generates a residual stress layer that is even deeper in magnitude than other surface treatments. Prabhakaran et al. [177] conducted a study to investigate the effect of laser shot peening on structural steel used in automobiles. The findings from high-cycle fatigue tests indicated that life was improved by 15 times. Rolling, which uses a rolling ball/wheel to roll the contact surface, has been shown to enhance surface mechanical properties. Qu et al. [178] reported that ultrasonic rolling treatment significantly improved the distribution of hardness and compressive residual stress, thereby increasing the rolling contact fatigue life. Some works [179, 180] indicate the high load-carrying capacity potential of gears produced by fine-blanking due to increased compressive stresses, while the production process is very cost-efficient. The surface finishing process results in a

Fig. 21 Gear surface manufacturing processes (number of stars represents potential to improve surface integrity).

smooth surface through reciprocal rolling and grinding between media and components [181], resulting in a reduction in surface roughness and an improvement in contact fatigue resistance [182]. Zhang et al. [183] experimentally reported that barrel finishing significantly decreases surface roughness and increases the surface compressive residual stress (SCRS) by approximately 500 MPa. The increase in fatigue resistance has been validated through gear contact fatigue tests [77, 79]. Thermal barrier coatings, which deposit ceramic materials onto component surfaces, provide a combination of high strength, high toughness, and high-temperature resistance. Moorthy and Shaw [184] tested gear contact fatigue with various coating processes, such as Balint C, BalinitC*, and CrN+IFLM. They discovered that the coated gears exhibit less severe pitting than those without coatings. Wu et al. [185] conducted a comprehensive evaluation of the effects of a DLC coating on gear bending fatigue, contact fatigue, and scuffing performance, and the results indicated that the DLC coating increased gear contact fatigue limits by 200 MPa.

Surface manufacturing processes such as shot peening, rolling treatment, laser shock peening, thermal barrier coating, particle peening, and surface finishing can significantly enhance gear contact fatigue performance. By introducing high compressive residual stress and increasing surface hardness, shot peening and rolling treatment are suitable for heavy-load applications such as wind turbines and heavy-duty truck gearboxes. Laser shock peening provides a greater depth of compressive residual stress, making it appropriate for large-module gears. Particle peening and surface finishing decrease surface roughness, which is ideal for high-speed and precision transmissions. Moreover, thermal barrier coatings are applicable in high-temperature environments such as aerospace gear transmissions.

Shot peening increases the surface roughness, whereas the hardening layer for surface finishing is shallow, which may cause unsatisfactory gear performance. To improve overall surface performance, composite manufacturing processes, including double shot peening, coating after grinding, and surface finishing after shot peening, are becoming the focus of future work. An investigation conducted by Kratzer et al. [186] revealed a significant improvement in contact fatigue resistance by a combination of shot peening and surface finishing processes. In addition, pre-shot peening processes that contribute to carbon atom diffusion before heat treatment [187] have also been investigated and validated. As shown in Fig. 22, Wang et al. [79] investigated the contact fatigue performance of 18CrNiMo7-6 gears with ten different manufacturing processes, including shot peening, double shot peening, fine particle peening, thermal

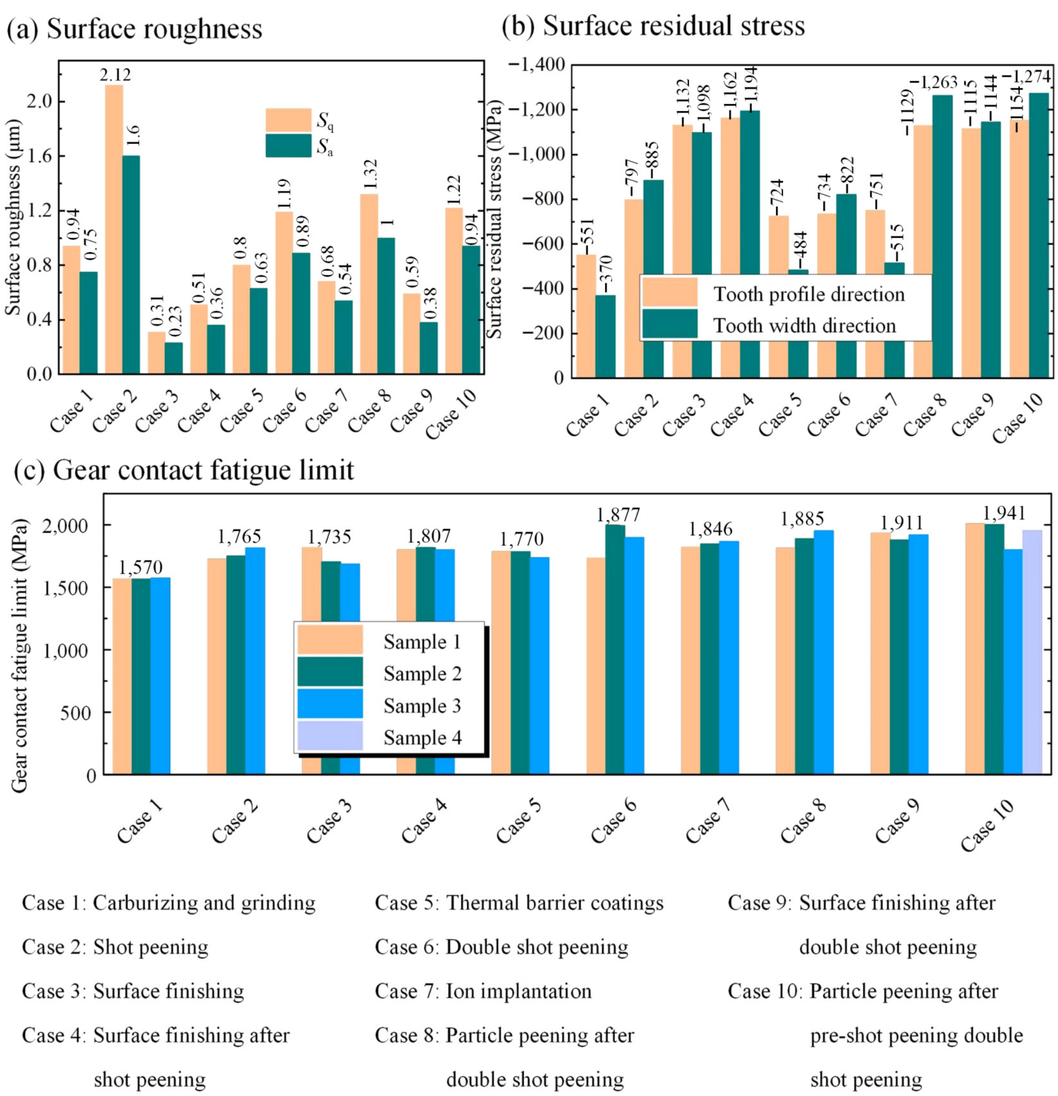

Fig. 22 Contact fatigue limits of 18CrNiMo7-6 gears with various manufacturing processes.

barrier coating, and ion implantation. The results revealed significant improvements in the contact fatigue limit compared with the benchmark grinding state. Among them, the composite process with pre-shot peening, double shot peening, and finally fine particle peening resulted in optimized surface morphology and mechanical properties. Its contact fatigue limit was 23.63% greater than that of the grinding process.

Table 3 provides a summary of the effects on gear contact fatigue. This method should be of interest to engineers when designing against gear contact fatigue.

Table 3 Effects on gear contact fatigue and anti-fatigue measures

Factor	Influence law	Improvement measure
Temperature	High temperatures can cause rupture of the oil film, an increase in friction coefficients, and gear material phase transformation or even softening.	Lower the oil temperature with cooling equipment, or improve surface morphology through surface finishing and coating.
Lubrication	Fatigue and friction properties can be altered by changes in lubrication method, type, and amount, which determine the lubrication film thickness and lubrication state.	The large amount of oil-injection lubrication with higher viscosity can achieve full-film lubrication.
Tooth profile	The profile errors caused by design and manufacturing tolerances result in uneven tooth surface loading.	Reasonable modification of tooth profile can improve contact stress distribution.
Surface morphology	Peak-to-peak contact generates stress concentration, and surface morphology also influences material microstructure evolution and oil film.	Surface finishing and particle shot peening can improve surface roughness and isotropy.
Residual stress	Tensile residual stress exacerbates the initiation and propagation of fatigue cracks, while compressive residual stress significantly improves fatigue strength.	High surface compressive residual stress can be obtained by surface finishing and particle shot peening, while laser shot peening and rolling treatment result in a greater depth of compressive residual stress.
Hardness gradient	High surface hardness and sufficient core toughness typically result in high wear and fatigue resistance.	High surface hardness and hardening depth can be achieved using shot peening, particle shot peening, or laser shot peening.

6 Conclusions and future work

The present work reviews analytical, numerical, and experimental investigations on gear contact fatigue. The gear contact fatigue failure mechanism was clarified. In addition, pivotal factors affecting gear contact fatigue were identified, and gear anti-fatigue design techniques were explored. The key conclusions can be summarized as follows:

(1) The interdependent factors of working conditions, gear geometry, and materials significantly affect gear contact fatigue performance. In-depth studies have been conducted on various aspects, such as lubrication, surface morphology, hardness gradient, residual stress, and material microstructure, to explore their effects on gear contact fatigue. Preliminary findings have revealed some of the underlying mechanisms of gear contact fatigue. On the basis of this understanding, different gear surface treatment methods, including shot peening, surface finishing, and coating, have been developed.

(2) Preliminary work has been conducted on advanced gear contact fatigue theories, resulting in high-precision models that consider surface integrity. Furthermore, innovative and effective testing methods, data processing techniques, and intelligent detection tools have been studied, offering crucial means to reveal the relationship between surface integrity and gear contact fatigue.

(3) Academia has successfully overcome some constraints of Hertzian contact theory, and data-driven models for gear contact fatigue considering surface integrity have been developed. This was achieved by using experimental or simulation data and artificial intelligence technologies to develop a prediction formula for gear contact fatigue. These findings provide valuable insights for achieving gear anti-fatigue design.

To further advance gear contact fatigue studies, the following areas are suggested:

(1) Although the significance of surface integrity has been acknowledged in gear contact fatigue, most fatigue models have focused only on single or limited factors while neglecting the intricate interactions among surface integrity parameters. As a result, there is a pressing need to establish multifactor and multiscale models for gear contact fatigue that can be extensively validated through experiments and engineering practices.

(2) Advanced gear devices used in modern aerospace, ships, robots, and vehicles often encounter extreme working conditions, such as high speed, heavy load, high temperature, and loss of lubrication. However, the lack of clear insights into operating behavior and failure mechanisms poses significant challenges to achieving high-reliability and long-life gear design. Therefore, there is an urgent need to develop gear fatigue theories, test methods, and design guidelines that are specifically tailored toward extreme operating conditions.

(3) While data-driven methods can provide reasonable predictions of gear contact fatigue properties, they have certain shortcomings. They are unable to consider physical damage, and their effectiveness is constrained by limitations in terms of the amount of data and authenticity. As a result, the development of physical-data hybrid models is anticipated to be a promising research area in the future. Such work [121] has emerged in the gear area in recent years.

Acknowledgements

This work was supported by the National Natural Science Foundation of China (No. 52322504).

Availability of data and materials

The data that support the findings of this study are available from the corresponding author upon reasonable request.

Declaration of competing interest

The authors have no competing interests to declare that are relevant to the content of this article.

References

[1] Wu J Z, Wei P T, Zhu C C, Zhang P, Liu H J. Development and application of high strength gears. *Int J Adv Manuf Tech* **132**(7): 3123–3148 (2024)

[2] Zhang B Y, Liu H J, Bai H Y, Zhu C C, Wu W. Ratchetting—

multiaxial fatigue damage analysis in gear rolling contact considering tooth surface roughness. *Wear* **428**: 137–146 (2019)

[3] Liu H L, Liu H J, Zhu C C, Sun Z D, Bai H Y. Study on contact fatigue of a wind turbine gear pair considering surface roughness. *Friction* **8**(3): 553–567 (2020)

[4] Aslantaş K, Taşgetiren S. A study of spur gear pitting formation and life prediction. *Wear* **257**(11): 1167–1175 (2004)

[5] König J, Felbermaier M, Tobie T, Stahl K. Tribological influencing factors on the formation of micropitting on case-hardened gears. *Schmiertechnik und Tribologie* **64**(2): 21–27 (2017)

[6] Liu H J, Liu H L, Zhu C C, Zhou Y. A review on micropitting studies of steel gears. *Coatings* **9**(1): 42 (2019)

[7] Chen D F, Zhu J Z, Liu H J, Wei P T, Mao T Y. Experimental investigation of the relation between the surface integrity and bending fatigue strength of carburized gears. *Sci China Technol Sc* **66**(1): 33–46 (2023)

[8] He H F, Zhou Y, Liu H L, Zhu C C, Xiao B, Zhang T H. Study on gear bending fatigue considering gradient characteristics: Numerical analysis and experiments. *Eng Fract Mech* **277**: 108983 (2023)

[9] Chen T M, Zhu C C, Liu H J, Wei P T, Zhu J Z, Xu Y Q. Simulation and experiment of carburized gear scuffing under oil jet lubrication. *Eng Fail Anal* **139**: 106406 (2022)

[10] Li R Z, Zhao Q H. *Gear Strength Design Data*. Beijing (China): China Machine Press, 1984.

[11] Li Z M, Yang X Z, Ling J S, Yang F Y, Wang L J. Analysis on the fore-invalidation of the automobile final reduction gear. *Acta Agric Univ Henan* **32**(2): 176–180 (1998) (in Chinese)

[12] Davies D P, Jenkins S L, Belben F R. Survey of fatigue failures in helicopter components and some lessons learnt. *Eng Fail Anal* **32**: 134–151 (2013)

[13] Zhou Y, Zhu C C, Bai H Y, Feng H B, Dai X W. Analytical study of tooth flank fracture in case-hardened gears considering non-metallic inclusion. *Eng Fail Anal* **138**: 106373 (2022)

[14] Terrin A, Dengo C, Meneghetti G. Experimental analysis of contact fatigue damage in case hardened gears for off-highway axles. *Eng Fail Anal* **76**: 10–26 (2017)

[15] Ristivojević M, Lučanin V, Dimić A, Mišković Ž, Burzić Z, Stamenić Z, Rackov M. Investigation of the heavy duty truck gear drive failure. *Eng Fail Anal* **144**: 106995 (2023)

[16] Johnson K L. One hundred years of Hertz contact. *P I Mech Eng* **196**(1): 363–378 (1982)

[17] Seabrook J B, Dudley D W. Results of a fifteen-year program of flexural fatigue testing of gear teeth. *J Eng Ind* **86**(3): 221–237 (1964)

[18] Switzerland-IOS. ISO 6336-2 Calculation of load capacity of spur and helical gears-part 2: Calculation of surface durability (pitting). IOS, 2006.

[19] Asi O. Fatigue failure of a helical gear in a gearbox. *Eng Fail Anal* **13**(7): 1116–1125 (2006)

[20] Switzerland-IOS. ISO 10825-1 Gears—Wear and damage to gear teeth, Part 1: Nomenclature and characteristics. IOS, 2022.

[21] Switzerland-IOS. ISO 10825-2 Gears—Wear and damage to gear teeth, Part 2: Supplementary information. IOS, 2022.

[22] Höhn B-R, Oster P, Tobie T, Witzig J. Micropitting on gears—fundamentals. In: Proceedings of the 17th International Colloquium Tribology, 2010.

[23] Vouaillat G, Noyel J P, Ville F, Kleber X, Rathery S. From hertzian contact to spur gears: Analyses of stresses and rolling contact fatigue. *Mech Ind* **20**(6): 626 (2019)

[24] Zhou Y, Zhu C C, Liu H J, Song C S, Li Z F. A numerical study on the contact fatigue life of a coated gear pair under EHL. *Ind Lubr Tribol* **70**(1): 23–32 (2018)

[25] Fernandes P J L, McDuling C. Surface contact fatigue failures in gears. *Eng Fail Anal* **4**(2): 99–107 (1997)

[26] Sharif K J, Evans H P, Snidle R W. Modelling of elastohydrodynamic lubrication and fatigue of rough surfaces: The effect of lambda ratio. *P I Mech Eng J—J-Eng* **226**(12): 1039–1050 (2012)

[27] Liu H L, Liu H J, Zhu C C, He H F, Wei P T. Evaluation of contact fatigue life of a wind turbine gear pair considering residual stress. *J Tribol* **140**(4): 041102 (2018)

[28] Li S, Kahraman A. A fatigue model for contacts under mixed elastohydrodynamic lubrication condition. *Int J Fatigue* **33**(3): 427–436 (2011)

[29] Li S, Anisetti A. A tribo-dynamic contact fatigue model for spur gear pairs. *Int J Fatigue* **98**: 81–91 (2017)

[30] Lundberg G, Palmgren A. Dynamic capacity of rolling bearings. *J Appl Mech* **16**(2): 165–172 (1949)

[31] Coy J J, Zaretsky E V. Life analysis of helical gear sets using Lundberg–Palmgren theory. *NASA technical note* NASA-TN-D-8045, Washington, USA, 1975.

[32] Zhang B Y, Liu H J, Wei P T, Guagliano M, Hou S W. A modified model of Lundberg–Palmgren rolling contact fatigue formula considering the effects of surface treatments. *Friction* **11**(10): 1922–1938 (2023)

[33] Ioannides E, Harris T A. A new fatigue life model for rolling bearings. *J Tribol* **107**(3): 367–377 (1985)

[34] Zaretsky E V, Poplawski J V, Miller C R. Rolling bearing life prediction—Past, present, and future. NASA/TM—2000-210529. Washington, USA, 2000.

[35] Switzerland-ISO. ISO 281 Rolling bearings: dynamic load ratings and rating life. IOS, 1990.

[36] Tallian T E. Simplified contact fatigue life prediction model: Part I: Review of published models. *J Tribol* **114**(2): 207–213 (1992)

[37] Wang W, Liu H J, Zhu C C, Du X S, Tang J Y. Effect of the residual stress on contact fatigue of a wind turbine carburized gear with multiaxial fatigue criteria. *Int J Mech Sci* **151**: 263–273 (2019)

[38] Wang W, Liu H J, Zhu C C, Wei P T, Tang J Y. Effects of microstructure on rolling contact fatigue of a wind turbine gear based on crystal plasticity modeling. *Int J Fatigue* **120**: 73–86 (2019)

[39] Liu H J, Liu H L, Zhu C C, Wei P T, Tang J Y. Tribological behavior of coated spur gear pairs with tooth surface roughness. *Friction* **7**(2): 117–128 (2019)

[40] Wei P T, Zhou H, Liu H J, Zhu C C, Wang W, Deng G Y. Modeling of contact fatigue damage behavior of a wind turbine carburized gear considering its mechanical properties and microstructure gradients. *Int J Mech Sci* **156**: 283–296 (2019)

[41] Pavlina E J, Van Tyne C J. Correlation of yield strength and tensile strength with hardness for steels. *J Mater Eng Perform* **17**(6): 888–893 (2008)

[42] Wang J, Ren L, Xie L Z, Xie H P, Ai T. Maximum mean principal stress criterion for three-dimensional brittle fracture. *Int J Solids Struct* **102–103**: 142–154 (2016)

[43] Chang K J. On the maximum strain criterion: A new approach to the angled crack problem. *Eng Fract Mech* **14**(1): 107–124 (1981)

[44] Lance R H, Robinson D N. A maximum shear stress theory of plastic failure of fiber-reinforced materials. *J Mech Phys Solids* **19**(2): 49–60 (1971)

[45] Yang W H. A generalized von Mises criterion for yield and fracture. *J Appl Mech* **47**(2): 297–300 (1980)

[46] Chaboche J L. Constitutive equations for cyclic plasticity and cyclic viscoplasticity. *Int J Plasticity* **5**(3): 247–302 (1989)

[47] Gao B J, Chen X, Chen G. Ratchetting and ratchetting boundary study of pressurized straight low carbon steel pipe under reversed bending. *Int J Pres Ves Pip* **83**(2): 96–106 (2006)

[48] Zhang B Y, Liu H J, Zhu C C, Ge Y B. Simulation of the fatigue-wear coupling mechanism of an aviation gear. *Friction* **9**(6): 1616–1634 (2021)

[49] Karolczuk A, Skibicki D, Pejkowski Ł. Evaluation of the Fatemi-Socie damage parameter for the fatigue life calculation with application of the Chaboche plasticity model. *Fatigue Fract Eng M* **42**(1): 197–208 (2019)

[50] Desimone H, Bernasconi A, Beretta S. On the application of Dang

Van criterion to rolling contact fatigue. *Wear* **260**(4–5): 567–572 (2006)

[51] Brown M W, Miller K J. A theory for fatigue failure under multiaxial stress–strain conditions. *P I Mech Eng* **187**(1): 745–755 (1973)

[52] Fatemi A, Socie D F. A critical plane approach to multiaxial fatigue damage including out-of-phase loading. *Fatigue Fract Eng M* **11**(3): 149–165 (1988)

[53] Wang W, Liu H J, Zhu C C, Sun Z D. Evaluation of contact fatigue life of a wind turbine carburized gear considering gradients of mechanical properties. *Int J Damage Mech* **28**(8): 1170–1190 (2019)

[54] Reis T, de Abreu Lima E, Bertelli F, dos Santos A A Jr. Progression of plastic strain on heavy-haul railway rail under random pure rolling and its influence on crack initiation. *Adv Eng Softw* **124**: 10–21 (2018)

[55] Jiang Y, Sehitoglu H. Modeling of cyclic ratchetting plasticity, part I: Development of constitutive relations. *J Appl Mech* **63**(3): 720–725 (1996)

[56] Benasciutti D, Sherratt F, Cristofori A. Recent developments in frequency domain multi-axial fatigue analysis. *Int J Fatigue* **91**: 397–413 (2016)

[57] Karolczuk A, Macha E. A review of critical plane orientations in multiaxial fatigue failure criteria of metallic materials. *Int J Fracture* **134**(3): 267–304 (2005)

[58] US-AGMA. AGMA 2101 Fundamental rating factors and calculation methods for involute spur and helical gear teeth. AGM, 2016.

[59] Germany-DIN. DIN 3990-2 Calculation of load capacity of cylindrical gear: Calculation of pitting resistance. DIN, 2016.

[60] China-The State Bureau of Quality and Technical Supervision. GB/T 3480-1997 Calculation methods of load capacity for involute cylindrical gears. The State Bureau of Quality and Technical Supervision, 1997.

[61] Switzerland-ISO. ISO 6336-5 Calculation of load capacity of spur and helical gears-part 5: Strength and quality of materials. ISO, 2003.

[62] Labath O A, Richter D. Comparison of rating trends in AGMA versus ISO. *Gear Technol* **21**(3): 56–63 (2004)

[63] Kawalec A, Wiktor J, Ceglarek D. Comparative analysis of tooth-root strength using ISO and AGMA standards in spur and helical gears with FEM-based verification. *J Mech Design* **128**(5): 1141–1158 (2006)

[64] Rinaldo J M. A comparison of current AGMA, ISO and API gear rating methods. *Gear Technol* **35**(5): 46–52 (2018)

[65] Germany-DIN. DIN 3990-16 Calculation of load capacity of cylindrical gears—Part 16: Determination of the micro-pitting load-carrying capacity of lubricants using FZG-test-method GT-C/8, 3/90. DIN, 2020.

[66] Sagraloff N, Tobie T, Stahl K. Suitability of the test results of micropitting tests acc. to FVA 54/7 for modern practical gear applications. *Eng Res* **86**(3): 471–481 (2022)

[67] Zhang L, Wang L. Optimization of site investigation program for reliability assessment of undrained slope using Spearman rank correlation coefficient. *Comput Geotech* **155**: 105208 (2023)

[68] Emerson R W. Causation and Pearson's correlation coefficient. *J Visual Impair Blin* **109**(3): 242–244 (2015)

[69] Durodola J F, Ramachandra S, Gerguri S, Fellows N A. Artificial neural network for random fatigue loading analysis including the effect of mean stress. *Int J Fatigue* **111**: 321–332 (2018)

[70] Agrawal A, Choudhary A. An online tool for predicting fatigue strength of steel alloys based on ensemble data mining. *Int J Fatigue* **113**: 389–400 (2018)

[71] Zhou R Z, Xing Z G, Wang H D, Piao Z Y, Huang Y F, Guo W L, Ma R B. Prediction of contact fatigue life of AT40 ceramic coating based on neural network. *Anti-Corros Method M* **67**(1): 83–100 (2020)

[72] Bénard C, Da Veiga S, Scornet E. Mean decrease accuracy for random forests: Inconsistency, and a practical solution via the Sobol-MDA. *Biometrika* **109**(4): 881–900 (2022)

[73] Hancock J T, Khoshgoftaar T M. CatBoost for big data: An interdisciplinary review. *J Big Data* **7**(1): 94 (2020)

[74] Greenacre M, Groenen P J F, Hastie T, D'Enza A I, Markos A, Tuzhilina E. Principal component analysis. *Nat Rev Method Prime* **2**(1): 100 (2022)

[75] Kuo Y, Yang T, Huang G W. The use of grey relational analysis in solving multiple attribute decision-making problems. *Comput Ind Eng* **55**(1): 80–93 (2008)

[76] Wu X L, Hu F. Analysis of ecological carrying capacity using a fuzzy comprehensive evaluation method. *Ecol Indic* **113**: 106243 (2020)

[77] Zhang X H, Wei P T, Parker R G, Liu G L, Liu H J, Wu S J. Study on the relation between surface integrity and contact fatigue of carburized gears. *Int J Fatigue* **165**: 107203 (2022)

[78] Zhou K, Sun X Y, Shi S W, Song K, Chen X. Machine learning-based genetic feature identification and fatigue life prediction. *Fatigue Fract Eng M* **44**(9): 2524–2537 (2021)

[79] Wang Q Z, Zhang X H, Wu J Z, Li Y, Wei P T, Liu H J. Research on contact fatigue limit prediction method of carburized gears based on catboost algorithm. *Chin J Theor Appl Mech* **56**(12): 3564–3576 (2024) (in Chinese)

[80] Xia S M, Li R S. Determination of load capabilities of lubricants by gear tester FZG. *Lubr Eng* **10**(1): 58–62+57 (1985) (in Chinese)

[81] Townsend D P, Coy J J, Zaretsky E V. Experimental and analytical load-life relation for AISI 9310 steel spur gears. *J Mech Design* **100**(1): 54–60 (1978)

[82] Information on https://www.highspeed-fzg.de

[83] Al-Tubi I S, Long H, Zhang J, Shaw B. Experimental and analytical study of gear micropitting initiation and propagation under varying loading conditions. *Wear* **328**: 8–16 (2015)

[84] Kleemola J, Lehtovaara A. Experimental simulation of gear contact along the line of action. *Tribol Int* **42**(10): 1453–1459 (2009)

[85] Patzer G, Woydt M, Shah R, Miller C, Iaccarino P. Test modes for establishing the tribological profile under slip-rolling. *Lubricants* **8**(5): 59 (2020)

[86] Matkovič S, Kalin M. Effects of slide-to-roll ratio and temperature on the tribological behaviour in polymer-steel contacts and a comparison with the performance of real-scale gears. *Wear* **477**: 203789 (2021)

[87] Savolainen M, Lehtovaara A. An approach to investigating subsurface fatigue in a rolling/sliding contact. *Int J Fatigue* **117**: 180–188 (2018)

[88] Merritt H E. Worm gear performance. *P I Mech Eng* **129**(1): 127–194 (1935)

[89] Meneghetti G, Terrin A, Giacometti S. A twin disc test rig for contact fatigue characterization of gear materials. *Procedia Struct Integr* **2**: 3185–3193 (2016)

[90] Ahlroos T, Ronkainen H, Helle A, Parikka R, Virta J, Varjus S. Twin disc micropitting tests. *Tribol Int* **42**(10): 1460–1466 (2009)

[91] Li Y, Wei P T, Xiang G, Jia C F, Liu H J. Gear contact fatigue life prediction based on transfer learning. *Int J Fatigue* **173**: 107686 (2023)

[92] Zhong B B, Song H L, Liu H J, Wei P T, Lu Z H. Loading capacity of POM gear under oil lubrication. *J Adv Mech Des Syst* **16**(1): JAMDSM0006 (2022)

[93] Germany-DIN. DIN ISO 14635 Gears—FZG test procedures—Part 1: FZG test method A/8, 3/90 for relative scuffing load-carrying capacity of oils. Deutsches Institut für Normung (DIN), 2016.

[94] Germany-CEC. CEC L-108 FZG pitting load carrying capacity test for gear oils. Gear Research Center, 2022.

[95] Germany-DGMK. DGMK 377 FZG slow speed sear test C/0, 05/90: 120/12, Gear Research Center, 1997.

[96] Chen T M, Wei P T, Zhu C C, Zeng P, Li D S, Parker R, Liu H J. Experimental investigation of gear scuffing for various tooth surface treatments. *Tribol T* **66**(1): 35–46 (2023)

[97] Information on https://www.mec.ed.tum.de/en/fzg/research-1/technical-equipment/

[98] Gao B, He Y Z, Woo W L, Gui Y T, Liu J, Hu Y H. Multidimensional tensor-based inductive thermography with multiple physical fields for offshore wind turbine gear inspection. *IEEE T Ind Electron* **63**(10): 6305–6315 (2016)

[99] Cameron Z A, Krantz T L. Statistical distribution of gear surface fatigue lives at high reliability. *Int J Fatigue* **167**: 107350 (2023)

[100] Lu Z H, Wei D, Wei P T, Liu H J, Yan H, Yu S X, Deng G Y. Contact fatigue performance and failure mechanisms of Fe-based small-module gears fabricated using powder metallurgy technique. *J Mater Res Technol* **26**: 1412–1427 (2023)

[101] Dobler A, Hergesell M, Tobie T, Stahl K. Increased tooth bending strength and pitting load capacity of fine-module gears. *Gear Technol* 48–53 (2016)

[102] Höhn B R, Stahl K, Schudy J, Tobie T, Zornek B. FZG rig-based testing of flank load-carrying capacity internal gears. *Gear Technol* 60–69 (2012)

[103] Xiang S, Qin Y, Zhu C C, Wang Y Y, Chen H Z. LSTM networks based on attention ordered neurons for gear remaining life prediction. *ISA T* **106**: 343–354 (2020)

[104] Höhn B-R, Winter H. Laboratories at work: Institute for machine elements, Gear Research Centre (FZG). *Tribotest* **3**(3): 325–340 (1997)

[105] Schnetzer P E, Pellkofer J, Stahl K. Calculation method for wear of steel-bronze rolling-sliding contacts relating to worm gears. *Eng Res* **87**(3): 961–971 (2023)

[106] Stahl K, Patel S V, Otto M, Sendlbeck S. Gear condition monitoring by augmenting measured transmission error data for gear damage and propagation estimation. *Int J Powertrains* **12**(3): 262–281 (2023)

[107] Lu Z H, Liu H J, Zhu C C, Yu G D, Zhong B B. Effects of lubrication and loading levels on POM gear durability performance. *China Mech Eng* **32**(17): 2047–2054 (2021) (in Chinese)

[108] Wei P, Chen T, Zhu C, Liu H, Li Yang, Lu Z. Intelligent gear monitoring system and method containing multi-dimensional information fusion. CN202211184197.X, Dec. 2022. (in Chinese)

[109] Tchankov D S, Vesselinov K V. Fatigue life prediction under random loading using total hysteresis energy. *Int J Pres Ves Pip* **75**(13): 955–960 (1998)

[110] Zhang O Q, Poirier J A, Barr J E. Modified Locati method in fatigue testing. *SAE Technical Paper*: 2003-01-0919 (2003)

[111] Bonaiti L, Geitner M, Tobie T, Gorla C, Stahl K. A comparison between two statistical methods for gear tooth root bending strength estimation starting from pulsator data. *Appl Scil* **13**(3): 1546 (2023)

[112] Gao J X, Xu R X, Wu Z F, Zhu P N. A general method for determining probabilistic S–N curve based on static strength data of material. *P I Mech Eng C—J Mec* **236**(9): 4862–4875 (2022)

[113] Hein M, Tobie T, Stahl K. Test method for time-scaled fatigue tests of gear transmission systems. *Eng Res* **81**(2): 291–297 (2017)

[114] Chen Y L. Method for compiling accelerated load spectrum of aviation gear transmission system considering fatigue-scuffing failure. Master Thesis. Chongqing (China): Chongqing University, 2024.

[115] Schijve J. A normal distribution or a Weibull distribution for fatigue lives. *Fatigue Fract Eng M* **16**(8): 851–859 (1993)

[116] Gope P C. Determination of sample size for estimation of fatigue life by using Weibull or log-normal distribution. *Int J Fatigue* **21**(8): 745–752 (1999)

[117] Barbosa J F, Correia J A, Freire R Jr, Zhu S P, De Jesus A M. Probabilistic S–N fields based on statistical distributions applied to metallic and composite materials: State of the art. *Adv Mech Eng* **11**(6): 1687814019870395 (2019)

[118] Gül Ç, Gürbüz R. Evaluation of fatigue performance of a fillet rolled diesel engine crankshaft. *Eng Fail Anal* **27**: 250–261 (2013)

[119] Jia C F, Wei P T, Lu Z H, Ye M, Zhu R, Liu H J. A novel prediction approach of polymer gear contact fatigue based on a WGAN-XGBoost model. *Fatigue Fract Eng M* **46**(6): 2272–2283 (2023)

[120] Liu H J, Li Y, Lu Z H, Wang Z R, Wang Z, Zeng X B. A unified estimation method for gear fatigue P–S–N curves and fatigue limits based on ensemble learning and data augmentation. *Eng Fract Mech* **298**: 109941 (2024)

[121] Li Y, Liu H J, Chen Y M, Chen D F. Probabilistic gear fatigue life prediction based on physics-informed transformer. *Expert Syst Appl* **249**: 123882 (2024)

[122] Mao T Y, Liu H J, Wang B B, Hou S W, Chen D F. Analysis of gear bending fatigue test based on hierarchical Bayesian model. *China Mech Eng* **32**(24): 3008–3015 (2021) (in Chinese)

[123] Mao T Y, Liu H J, Wei P T, Chen D F, Zhang P, Liu G Q. An improved estimation method of gear fatigue strength based on sample expansion and standard deviation correction. *Int J Fatigue* **161**: 106887 (2022)

[124] Lu Z H, Reitschuster S, Tobie T, Stahl K, Liu H J, Hu X L. Contact fatigue life prediction of PEEK gears based on CTAB-GAN data augmentation. *Eng Fract Mech* **312**: 110639 (2024)

[125] Liu H L, Liu H J, Zhu C C, Ge Y B. Influence of load spectrum on contact fatigue damage of a case carburized wind turbine gear. *Eng Fail Anal* **119**: 105005 (2021)

[126] Zhang Y M, Liu Y Z. Research on the rolling contact fatigue life of the bearing considering the friction effect. *P I Mech Eng C—J Mec* **235**: 2238–2264 (2021)

[127] Olver A. Temperature and lubrication of gears in high speed transmissions. In: Proceedings of the IMechE Seminar on Lubricants and Lubrication Systems, 1993: 1–11.

[128] Moss J, Kahraman A, Wink C. An experimental study of influence of lubrication methods on efficiency and contact fatigue life of spur gears. *J Tribol* **140**(5): 051103 (2018)

[129] Winter H, Knauer G. Influence of lubricant and operating temperature on the pitting load carrying capacity of case-hardened gears, Part 1. *Drive Technol* **29**(8): 65–70 (1990) (in German)

[130] Höhn B R, Oster P, Radev T, Tobie T. The "practice relevant pitting test"—A new improved test method to evaluate the influence of lubricants on the pitting load capacity of case carburized gears. *J ASTM Int* **4**(9): 1–9 (2007)

[131] Sagraloff N, Dobler A, Tobie T, Stahl K, Ostrowski J. Development of an oil free water-based lubricant for gear applications. *Lubricants* **7**(4): 33 (2019)

[132] Sagraloff N, Winkler K J, Tobie T, Stahl K, Folland C, Asam T. Investigations on the scuffing and wear characteristic performance of an oil-free water-based lubricant for gear applications. *Lubricants* **9**(3): 24 (2021)

[133] Gebremariam M, Thakur A, Leake E, Tilahun D. Effect of change of contact ratio on contact fatigue stress of involute spur gears. *Int J Curr Eng Technol* **8**(3): 719–731 (2018)

[134] Guilbault R, Lalonde S. Tip relief designed to optimize contact fatigue life of spur gears using adapted PSO and Firefly algorithms. *SN Appl Sci* **3**(1): 66 (2021)

[135] Qin W J, Guan C Y. An investigation of contact stresses and crack initiation in spur gears based on finite element dynamics analysis. *Int J Mech Sci* **83**: 96–103 (2014)

[136] Geitner M, Zornek B, Tobie T, Stahl K. Investigations on the pitting load capacity of internal spur and helical gears. *Forsch Ingenieurwes* **83**(3): 553–561 (2019)

[137] Otto M, Weinberger U, Stahl K. Full contact analysis versus standard load capacity calculation for cylindrical gears. *Gear Technol* 84–89 (2018)

[138] Geitner M, Preintner S, Tobie T, Stahl K. Simulation study on the tribological characteristics in the meshing contact in the context of the load carrying capacity calculation of internal gears with unbalanced sliding conditions. *Forsch Ingenieurwes* **87**(3): 821–832 (2023)

[139] Ichimaru K, Nakajima A, Hirano F. Effect of asperity interaction on pitting in rollers and gears. *J Mech Design* **103**(2): 482–491 (1981)

[140] Zhang B Y, Liu H J, Zhu C C, Li Z. Numerical simulation of competing mechanism between pitting and micro-pitting of a wind

turbine gear considering surface roughness. *Eng Fail Anal* **104**: 1–12 (2019)
[141] Klein M A. An experimental investigation of materials and surface treatments on gear contact fatigue life. M.S. Thesis. Columbus (USA): The Ohio State University, 2009.
[142] Zhou H, Wei P T, Liu H J, Zhu C C, Wang W. Crystal elasticity analysis of contact fatigue behavior of a wind turbine gear. *J Mech Sci Technol* **33**(10): 4791–4802 (2019)
[143] Fuchs D, Fiederling E, Tobie T, Stahl K. Investigations on the hardness and grain size of gears made out of ultra-clean gear steels after case-hardening. *HTM—J Heat Treat Mat* **77**(1): 53–69 (2022)
[144] Rommel S, Fuchs D, Blum T, Tobie T, Stahl K. Influence of different pre-heat treatments on the grain size in the core region of ultra-clean gear steels. *HTM—J Heat Treat Mat* **77**(4): 284–297 (2022)
[145] Tobie T, Hippenstiel F, Mohrbacher H. Optimizing gear performance by alloy modification of carburizing steels. *Metals* **7**(10): 415 (2017)
[146] Zhu D, Wang F X, Cai Q G, Zheng M X, Cheng Y Q. Effect of retained austenite on rolling element fatigue and its mechanism. *Wear* **105**(3): 223–234 (1985)
[147] Roy S, Ooi G T C, Sundararajan S. Effect of retained austenite on micropitting behavior of carburized AISI 8620 steel under boundary lubrication. *Materialia* **3**: 192–201 (2018)
[148] Güntner C, Tobie T, Stahl K. Alternative microstructures and their influence on mechanical properties of case-hardened gears. *Forsch Ingenieurwes* **81**(2): 245–251 (2017)
[149] Blech N, Güntner C, Schurer S, Steinbacher M, Tobie T, Stahl K. Material influence on mechanical properties of gears with alternative microstructures. *Forsch Ingenieurwes* **87**(2): 593–603 (2023)
[150] Liu H L, Liu H J, Bocher P, Zhu C C, Sun Z D. Effects of case hardening properties on the contact fatigue of a wind turbine gear pair. *Int J Mech Sci* **141**: 520–527 (2018)
[151] Li W, Deng S, Liu B S. Experimental study on the influence of different carburized layer depth on gear contact fatigue strength. *Eng Fail Anal* **107**: 104225 (2020)
[152] Wang W, Liu H J, Zhu C C, Bocher P, Liu H L, Sun Z D. Evaluation of rolling contact fatigue of a carburized wind turbine gear considering the residual stress and hardness gradient. *J Tribol* **140**(6): 061401 (2018)
[153] Ooi G T C, Roy S, Sundararajan S. Investigating the effect of retained austenite and residual stress on rolling contact fatigue of carburized steel with XFEM and experimental approaches. *Mater Sci Eng A—Struct* **732**: 311–319 (2018)
[154] Koenig J, Koller P, Tobie T, Stahl K. Influence of additional surface finishing to the material properties and the flank load carrying capacity of case-hardened gears with grinding burn. *J Adv Mech Des Syst* **11**(6): JAMDSM0075 (2017)
[155] Lu Z H, Liu H J, Zhu C C, Song H L, Yu G D. Identification of failure modes of a PEEK-steel gear pair under lubrication. *Int J Fatigue* **125**: 342–348 (2019)
[156] Lu Z H, Liu H J, Wei P T, Zhu C C, Xin D, Shen Y Q. The effect of injection molding lunker defect on the durability performance of polymer gears. *Int J Mech Sci* **180**: 105665 (2020)
[157] Yu G D, Liu H J, Mao K, Zhu C C, Lu Z H. Examination on the wear process of polyformaldehyde gears under dry and lubricated conditions. *Friction* **9**(3): 538–550 (2021)
[158] Lu Z H, Liu H J, Zhang R H, Zhu C C, Shen Y Q, Xin D. The simulation and experiment research on contact fatigue performance of acetal gears. *Mech Mater* **154**: 103719 (2021)
[159] Hasl C, Illenberger C, Oster P, Tobie T, Stahl K. Potential of oil-lubricated cylindrical plastic gears. *J Adv Mech Des Syst* **12**(1): JAMDSM0016 (2018)
[160] Illenberger C M, Tobie T, Stahl K. Flank load carrying capacity of oil-lubricated high performance plastic gears. *Forsch Ingenieurwes* **83**(3): 545–552 (2019)
[161] Illenberger C M, Tobie T, Stahl K. High-performance plastic gears. In: *Recent Advances in Gearing: Scientific Theory and Applications*. Radzevich S P, Ed. Berlin (Germany): Springer, 2022: 143–182.
[162] Illenberger C M, Tobie T, Stahl K. Operating behavior and performance of oil-lubricated plastic gears. *Forsch Ingenieurwes* **86**(3): 557–565 (2022)
[163] Reitschuster S, Illenberger C M, Tobie T, Stahl K. Application of high performance polymer gears in light urban electric vehicle powertrains. *Forsch Ingenieurwes* **86**(4): 683–691 (2022)
[164] Hoja S, Hoffmann F, Zoch H W, Schurer S, Tobie T, Stahl K. Design of deep nitriding treatments for gears. *HTM—J Heat Treat Mat* **70**(6): 276–285 (2015) (in German)
[165] Sitzmann A, Hoja S, Schurer S, Tobie T, Stahl K. Deep nitriding: Contact and bending strength of gears with increased nitriding hardening depth. *Forsch Ingenieurwes* **86**(3): 649–659 (2022)
[166] Cermak H, Dobler F, Nadolski D, Tobie T, Steinbacher M, Stahl K, Zoch H W. Influence of base material, tempered condition and hardening pattern on the residual stress profile of induction hardened gears. *Forsch Ingenieurwes* **83**(3): 571–577 (2019)
[167] Cermak H, Tobie T, Stahl K. Flame and induction hardening–an advantageous alternative to case hardening for large size gears? *HTM—J Heat Treat Mat* **77**(2): 112–126 (2022)
[168] Boniardi M, D'Errico F, Tagliabue C. Influence of carburizing and nitriding on failure of gears–A case study. *Eng Fail Anal* **13**(3): 312–339 (2006)
[169] Wu J Z, Liu H J, Wei P T, Lin Q J, Zhou S S. Effect of shot peening coverage on residual stress and surface roughness of 18CrNiMo7-6 steel. *Int J Mech Sci* **183**: 105785 (2020)
[170] Wu J Z, Liu H J, Wei P T, Zhu C C, Lin Q J. Effect of shot peening coverage on hardness, residual stress and surface morphology of carburized rollers. *Surf Coat Tech* **384**: 125273 (2020)
[171] Wu J Z, Wei P T, Liu H J, Zhang B Y, Tao G B. Effect of shot peening intensity on surface integrity of 18CrNiMo7-6 steel. *Surf Coat Tech* **421**: 127194 (2021)
[172] Lin Q J, Liu H J, Zhu C C, Chen D F, Zhou S S. Effects of different shot peening parameters on residual stress, surface roughness and cell size. *Surf Coat Tech* **398**: 126054 (2020)
[173] Lin Q J, Liu H J, Zhu C C, Parker R G. Investigation on the effect of shot peening coverage on the surface integrity. *Appl Surf Sci* **489**: 66–72 (2019)
[174] Li W, Liu B S. Experimental investigation on the effect of shot peening on contact fatigue strength for carburized and quenched gears. *Int J Fatigue* **106**: 103–113 (2018)
[175] Townsend D P. Improvement in surface fatigue life of hardened gears by high-intensity shot peening. In: Proceeding of the ASME Design Technical Conferences—6th International Power Transmission and Gearing Conference: Advancing Power Transmission Into the 21st Century, 1992: 643–649.
[176] Liu X, Liu J X, Zuo Z X, Zhang H Y. Effects of shot peening on fretting fatigue crack initiation behavior. *Materials* **12**(5): 743 (2019)
[177] Prabhakaran S, Kalainathan S, Shukla P, Vasudevan V K. Residual stress, phase, microstructure and mechanical property studies of ultrafine bainitic steel through laser shock peening. *Opt Laser Technol* **115**: 447–458 (2019)
[178] Qu S G, Hu X F, Lu F, Lai F Q, Liu H P, Zhang Y L, Li X Q. Rolling contact fatigue properties of ultrasonic surface rolling treated 25CrNi$_2$MoV steel under different lubricant viscosities. *Int J Fatigue* **142**: 105970 (2021)
[179] Stahl J, Müller D, Tobie T, Golle R, Volk W, Stahl K. Residual stresses in parts manufactured by near-net-shape-blanking. *Prod Eng Res Dev* **13**(2): 181–188 (2019)
[180] Nürnberger A, Müller D, Martinitz L, Hartmann C, Tobie T, Stahl K, Volk W. Advantages in the production of power transmitting gears by fineblanking. *Int J Adv Manuf Tech* **128**(9): 4413–4425 (2023)
[181] Li W H, Yang S Q, Yang S C, Chen H L. Theoretic analysis and simulation on horizontal spindle barrel finishing. *Key Eng Mater* **416**: 332–336 (2009)

[182] Zhang J, Shaw B A. The effect of superfinishing on the contact fatigue of case carburised gears. *Appl Mech Mater* **86**: 348–351 (2011)

[183] Zhang X H, Liu H J, Wu S J, Li G M, Wei P T. Experimental investigation on the effect of barrel finishing processes on surface integrity of 18CrNiMo7-6 carburized rollers. *P I Mech Eng E—J Pro* **236**(5): 2095–2105 (2022)

[184] Moorthy V, Shaw B A. Contact fatigue performance of helical gears with surface coatings. *Wear* **276**: 130–140 (2012)

[185] Wu J Z, Wei P T, Liu G Q, Chen D F, Zhang X H, Chen T M, Liu H J. A comprehensive evaluation of DLC coating on gear bending fatigue, contact fatigue, and scuffing performance. *Wear* **536**: 205177 (2024)

[186] Kratzer D, König J, Tobie T, Stahl K. Effects of different shot peening treatments in combination with a superfinishing process on the surface durability of case-hardened gears. *Gear Technol* 58–65 (2021)

[187] Wu J Z, Wei P T, Liu H J, Zhang X H, He Z Q, Deng G Y. Evaluation of pre-shot peening on improvement of carburizing heat treatment of AISI 9310 gear steel. *J Mater Res Technol* **18**: 2784–2796 (2022)

Huaiju Liu is currently working as a professor in the State Key Laboratory of Mechanical Transmission for Advanced Equipment, Chongqing University, China. He received his Ph.D. degree from the University of Warwick, UK, in 2013. His research fields include intelligent design of mechanical transmission.

Xiuhua Zhang has been studying as a Ph.D. student in the State Key Laboratory of Mechanical Transmission for Advanced Equipment, Chongqing University, China, since 2022. His current research focuses on gear contact fatigue and high-power-density transmission design.

Michael Geitner is currently working as the head of Worm and Bevel Gears Department, Gear Research Center (FZG), Technical University of Munich, Germany. His research fields include fatigue life analysis of mechanical elements.

Thomas Tobie is currently working as a head of Load Carrying Capacity of the Cylindrical Gears Department at Gear Research Center (FZG), Technical University of Munich, Germany. His research fields include gear materials, heat treatment, gear lubricants, and gear load carrying capacity.

Karsten Stahl is currently working as the director of the Gear Research Center (FZG), Technical University of Munich, Germany. His main research interests are drive components, such as gears, synchronizers, multidisc clutches, rolling bearings, and electromechanical drive systems.

Caichao Zhu is currently working as a professor in the State Key Laboratory of Mechanical Transmission for Advanced Equipment, Chongqing University, China. He received his Ph.D. degree from Chongqing University, China, in 1998. His research is related mainly to the intelligent design and dynamic analysis of transmission systems.